

This discussion paper is/has been under review for the journal Biogeosciences (BG).  
Please refer to the corresponding final paper in BG if available.

# A new mechanistic framework to predict OCS fluxes from soils

J. Ogée<sup>1</sup>, J. Sauze<sup>1</sup>, J. Kesselmeier<sup>2</sup>, B. Genty<sup>3</sup>, H. Van Diest<sup>2</sup>, T. Launois<sup>1</sup>, and L. Wingate<sup>1</sup>

<sup>1</sup>INRA, UMR 1391 ISPA, 33140 Villenave d'Ornon, France

<sup>2</sup>Max Planck Institute for Chemistry, Biogeochemistry Department, Mainz, Germany

<sup>3</sup>CNRS/CEA/Aix-Marseille University, UMR 6191 BVME, Saint-Paul-lez-Durance, France

Received: 27 August 2015 – Accepted: 3 September 2015 – Published: 22 September 2015

Correspondence to: J. Ogée (jerome.ogee@bordeaux.inra.fr)

Published by Copernicus Publications on behalf of the European Geosciences Union.

BGD

12, 15687–15736, 2015

A new mechanistic framework to predict OCS fluxes from soils

J. Ogée et al.

[Title Page](#)

[Abstract](#)

[Introduction](#)

[Conclusions](#)

[References](#)

[Tables](#)

[Figures](#)

[◀](#)

[▶](#)

[◀](#)

[▶](#)

[Back](#)

[Close](#)

[Full Screen / Esc](#)

[Printer-friendly Version](#)

[Interactive Discussion](#)



## Abstract

Estimates of photosynthetic and respiratory fluxes at large scales is needed to improve our predictions of the current and future global CO<sub>2</sub> cycle. Carbonyl sulphide (OCS) is the most abundant sulphur gas in the atmosphere and has been proposed as a new tracer of photosynthesis (GPP), as the uptake of OCS from the atmosphere is dominated by the activity of carbonic anhydrase (CA), an enzyme abundant in leaves that also catalyses CO<sub>2</sub> hydration during photosynthesis. But soils also exchange OCS with the atmosphere which complicates the retrieval of GPP from atmospheric budgets. Indeed soils can take up large amounts of OCS from the atmosphere as soil microorganisms also contain CA, and OCS emissions from soils have been reported in agricultural fields or anoxic soils. To date no mechanistic framework exists to describe this exchange of OCS between soils and the atmosphere but empirical results, once upscaled to the global scale, indicate that OCS consumption by soils dominates over production and its contribution to the atmospheric budget is large, at about one third of the OCS uptake by vegetation, with also a large uncertainty. Here, we propose a new mechanistic model of the exchange of OCS between soils and the atmosphere that builds on our knowledge of soil CA activity from CO<sub>2</sub> oxygen isotopes. In this model the OCS soil budget is described by a first-order reaction-diffusion-production equation, assuming that the hydrolysis of OCS by CA is total and irreversible. Using this model we are able to explain the observed presence of an optimum temperature for soil OCS uptake and show how this optimum can shift to cooler temperatures in the presence of soil OCS emissions. Our model can also explain the observed optimum with soil moisture content previously described in the literature as a result of diffusional constraints on OCS hydrolysis. These diffusional constraints are also responsible for the response of OCS uptake to soil weight and depth observed previously. In order to simulate the exact OCS uptake rates and patterns observed on several soils collected from a range of biomes, different CA activities had to be evoked in each soil type, coherent with expected physiological levels of CA in soil microbes and with CA activities derived from

[Title Page](#)

[Abstract](#)

[Introduction](#)

[Conclusions](#)

[References](#)

[Tables](#)

[Figures](#)

◀

▶

◀

▶

[Back](#)

[Close](#)

[Full Screen / Esc](#)

[Printer-friendly Version](#)

[Interactive Discussion](#)



CO<sub>2</sub> isotope exchange measurements, given the differences in affinity of CA for both trace gases. Our model can also be used to help upscale laboratory measurements to the plot or the region. Several suggestions are given for future experiments in order to test the model further and allow a better constraint on the large-scale OCS fluxes from both oxic and anoxic soils.

## 1 Introduction

The terrestrial biosphere is, with the ocean, the largest sink in the global atmospheric CO<sub>2</sub> budget, with a very large year-to-year variability (e.g., Gurney and Eckels, 2011). Yet there is a scarcity of observations on how photosynthesis (GPP) and respiration over land respond individually to warmer temperatures, increasing atmospheric CO<sub>2</sub> mixing ratios and changes in water availability (Beer et al., 2010; Frankenberg et al., 2011; Welp et al., 2011; Wingate et al., 2009). Obtaining new observational constraints of these two opposing land CO<sub>2</sub> gross fluxes at large scales is key to improve our models of the land C sink and provide robust projections of the atmospheric CO<sub>2</sub> budget and future climate (Friedlingstein et al., 2006; Piao et al., 2013).

In this context, additional tracers such as carbonyl sulphide (OCS), an analogue of CO<sub>2</sub> in many respects, could be very useful (Berry et al., 2013; Campbell et al., 2008; Kettle et al., 2002; Montzka et al., 2007). Indeed, the uptake rate of OCS by foliage is strongly related to GPP (Sandoval-Soto et al., 2005; Stimler et al., 2010), or more generally to the rate of CO<sub>2</sub> transfer into foliage (Seibt et al., 2010; Wohlfahrt et al., 2011). This is because both OCS and CO<sub>2</sub> molecules diffuse into foliage through the same stomatal pores and through mesophyll cells where they get rapidly hydrated in an enzymatic reaction with carbonic anhydrase (CA) (Beer et al., 2010; Frankenberg et al., 2011; Protoschill-Krebs and Kesselmeier, 1992; Welp et al., 2011; Wingate et al., 2009). However, unlike CO<sub>2</sub> that is reversibly hydrated and interconverted into bicarbonate, OCS molecules are irreversibly hydrolysed (Elliott et al., 1989) and are not expected to diffuse back to the atmosphere, given the high affinity of CA towards OCS

BGD

12, 15687–15736, 2015

[Title Page](#)

[Abstract](#)

[Introduction](#)

[Conclusions](#)

[References](#)

[Tables](#)

[Figures](#)

◀

▶

◀

▶

[Back](#)

[Close](#)

[Full Screen / Esc](#)

[Printer-friendly Version](#)

[Interactive Discussion](#)



and the high activity of CA usually found in leaves (Protoschill-Krebs et al., 1996; Stimmer et al., 2012).

Carbonic anhydrase is also widespread in diverse species from the Archaea, Bacteria, Fungi and Algae domains (Smith et al., 1999), so that OCS uptake can theoretically take place in soils. Several field studies provide support for this by showing that soils generally act as an OCS sink when measured at ambient concentrations (Castro and Galloway, 1991; Kuhn et al., 1999; J. Liu et al., 2010; Steinbacher et al., 2004; White et al., 2010; Yi et al., 2007) and that the uptake rate is reduced when the soil is autoclaved (Bremner and Banwart, 1976). Kesselmeier et al. (1999) also observed a significant (> 50 %) reduction of the OCS uptake rate in soil samples after adding ethoxyzolamide, one of the most efficient known CA inhibitors (e.g., Isik et al., 2009; Syrjänen et al., 2013). This finding strongly supports the idea that OCS uptake by soils is dominated by soil CA activity.

Soils can also emit OCS into the atmosphere as reported in some agricultural fields (Maseyk et al., 2014; Whelan and Rhew, 2015) or in anoxic soils (Devai and Delaune, 1995; Mello and Hines, 1994; Whelan et al., 2013; Yi et al., 2008) but the exact mechanisms for such emissions are still unclear (Mello and Hines, 1994; Whelan and Rhew, 2015). At the global scale, OCS consumption by soils seems to dominate over production and its contribution to the atmospheric budget is large, at about one third of the OCS uptake by vegetation, with also a large uncertainty (Berry et al., 2013; Kettle et al., 2002; Launois et al., 2015).

This large uncertainty in the OCS exchange rate from soils is partly caused by the variety of approaches used to obtain a global estimate of this flux. Kettle et al. (2002) assumed soil OCS fluxes responded to soil surface temperature and moisture only and used a parameterisation derived by Kesselmeier et al. (1999) from incubation measurements performed on a single agricultural soil in Germany. They recognised the limitation of such parameterisation and also noted the important role of some intrinsic properties of the soil and particularly its redox potential (Devai and Delaune, 1995) but did not account for it in their analysis. More recent approaches have assumed that

[Title Page](#)[Abstract](#)[Introduction](#)[Conclusions](#)[References](#)[Tables](#)[Figures](#)[◀](#)[▶](#)[◀](#)[▶](#)[Back](#)[Close](#)[Full Screen / Esc](#)[Printer-friendly Version](#)[Interactive Discussion](#)

the OCS flux from soils is proportional to other soil–air trace gas fluxes, such as heterotrophic (microbial) respiration (Berry et al., 2013) or the H<sub>2</sub> deposition rate (Launois et al., 2015). Experimental evidence that supports such scaling between different trace gas fluxes is however scarce and with mixed results. In summary, all the approaches to estimate soil OCS fluxes at large scales remain essentially empirical or based on hypotheses that are largely un-validated. Given the supposedly important contribution of soils in the global OCS atmospheric budget, it becomes apparent that a deeper understanding of this flux and its underlying mechanisms is urgently needed. Until then estimating global GPP using OCS as an additional tracer of the carbon cycle remains elusive.

A plethora of process-based models exist that describe the transport and fate of trace gases in porous media (Falta et al., 1989; Olesen et al., 2001). Transport processes are fairly well understood and similar between different trace gases. On the other hand the processes responsible for the emission or destruction are usually quite unique, i.e., specific to each trace gas. The main difficulty then resides in understanding these emission and destruction processes. Very recently Sun et al. (2015) proposed parameterisations of OCS emission and destruction in soils. However their parameterisations remain largely empirically-based and lack important drivers such as soil pH or redox potential. In this paper we propose a mechanistic framework to describe OCS uptake and release from soil surfaces, based on our current understanding of OCS biogeochemistry in soils. Our model includes OCS diffusion and advection through the soil matrix, OCS dissolution and hydrolysis in soil water and OCS production. Soil microbial activity contributes to OCS hydrolysis, through a pseudo first order CA-catalysed chemical reaction rate that varies with soil temperature and moisture, pH and CA concentration. OCS production, either abiotic or biotic, is also accounted for using a simple  $Q_{10}$  type temperature response modulated by the soil redox potential. Using the model we explore the theoretical response of OCS fluxes to soil water content, soil temperature, soil depth and soil pH. We also evaluate our model against observed soil OCS uptake rates and patterns from the literature and discuss how the CA-catalysed reac-

## A new mechanistic framework to predict OCS fluxes from soils

J. Ogée et al.

[Title Page](#)

[Abstract](#)

[Introduction](#)

[Conclusions](#)

[References](#)

[Tables](#)

[Figures](#)

[◀](#)

[▶](#)

[◀](#)

[▶](#)

[Back](#)

[Close](#)

[Full Screen / Esc](#)

[Printer-friendly Version](#)

[Interactive Discussion](#)



tion rates for each soil type can be reconciled with those typically observed for CO<sub>2</sub> hydration, given the differences in specificity of CA for OCS and CO<sub>2</sub>.

## 2 Model description

### 2.1 Partitioning of OCS in the different soil phases

5 Carbonyl sulphide, like any other trace gas, can be present in the soil matrix in three forms: (1) vaporised in the air-filled pore space, (2) dissolved in the water-filled pore space or (3) adsorbed on the surface of the soil matrix (mineral and organic matter solid particles). The total OCS concentration  $C_{\text{tot}}$  (mol m<sup>-3</sup>) is thus the sum of the OCS concentration in each phase weighted by their volumetric content:  $C_{\text{tot}} = \varepsilon_a C + \theta C_l + \rho_b C_s$  where  $\varepsilon_a$  (m<sup>3</sup> air m<sup>-3</sup> soil) is the volumetric air content,  $\theta$  (m<sup>3</sup> water m<sup>-3</sup> soil) is the volumetric water content,  $\rho_b$  (kg m<sup>-3</sup>) is soil bulk density,  $C$  and  $C_l$  (mol m<sup>-3</sup>) denote OCS concentration in soil air and liquid water respectively and  $C_s$  (mol kg<sup>-1</sup>) denotes the OCS concentration adsorbed on the soil matrix.

10 In the following we will assume full equilibrium between the three phases. We will also assume linear sorption/desorption behaviour (a fair assumption at ambient OCS concentrations), so that  $C_l$  and  $C_s$  can be linearly related to  $C$ :  $C_l = BC$  where  $B$  (m<sup>3</sup> water m<sup>-3</sup> air) is the solubility of OCS in water and  $C_s = (K_{\text{sg}} + BK_{\text{sw}})C$  where  $K_{\text{sg}}$  (m<sup>3</sup> air kg<sup>-1</sup> soil) and  $K_{\text{sw}}$  (m<sup>3</sup> water kg<sup>-1</sup> soil) are the solid/vapour and solid/liquid partitioning coefficients, respectively (Olesen et al., 2001). The solubility  $B$  is related to 15 Henry's law constant  $K_H$  (mol m<sup>-3</sup> Pa<sup>-1</sup>):  $B = K_H RT$  where  $R = 8.31446 \text{ J mol}^{-1} \text{ K}^{-1}$  is the ideal gas constant and  $T$  (K) is soil water temperature. It has been shown that  $K_H$  was fairly independent of pH (at least for pH = 9, see De Bruyn et al., 1995; Elliott et al., 1989) but decreased with temperature and salinity (De Bruyn et al., 1995; Elliott et al., 1989). In the following we will use the parameterisation of Wilhelm et al. (1977) 20 assuming low salinity levels in the soil:  $K_H = 0.021 \exp[24900/R(1/T - 1/298.15)]$ . We 25

12, 15687–15736, 2015

BGD

A new mechanistic framework to predict OCS fluxes from soils

J. Ogée et al.

<a href="#">Title Page</a>	
<a href="#">Abstract</a>	<a href="#">Introduction</a>
<a href="#">Conclusions</a>	<a href="#">References</a>
<a href="#">Tables</a>	<a href="#">Figures</a>
<a href="#">◀</a>	<a href="#">▶</a>
<a href="#">◀</a>	<a href="#">▶</a>
<a href="#">Back</a>	<a href="#">Close</a>
<a href="#">Full Screen / Esc</a>	
<a href="#">Printer-friendly Version</a>	
<a href="#">Interactive Discussion</a>	



preferred this expression rather than the more recent expression proposed by DeBruyn et al. (1995) that was based on one single dataset rather than a compilation of multiple datasets. The difference between the two expressions is shown in Fig. 1a.

Expressions of  $K_{sg}$  and  $K_{sl}$  for OCS are currently not available. For organic vapours it has been shown that  $K_{sl}$  is well correlated with soil characteristics such as C content (Petersen et al., 1995), specific surface area or clay content (Yamaguchi et al., 1999), and that  $K_{sg}$  is usually significant at soil water contents corresponding to less than five molecular layers of water coverage (Petersen et al., 1995). In this range of soil moisture, direct chemical adsorption onto dry mineral surfaces dominates and can increase the adsorption capacity of soils by several orders of magnitude. For these organic vapours the relationship of  $K_{sg}$  with soil moisture can be related to soil specific surface area (Petersen et al., 1995) or clay content (Yamaguchi et al., 1999). However these relationships obtained for organic vapours are unlikely applicable for OCS because the adsorption mechanisms may be completely different. Liu and colleagues have estimated OCS adsorption capacities of several mineral oxides and found that quartz ( $SiO_2$ ) and anatase ( $TiO_2$ ) did not adsorb OCS but other oxides with higher basicity adsorbed, reversibly or not, rather large quantities of OCS (Liu et al., 2008, 2010a, 2009). They also recognised that these estimates of the adsorption capacity of the minerals were an upper limit owing to the competitive adsorption of other gases such as  $CO_2$ ,  $H_2O$  and  $NO_x$  that occur in the real Earth's atmosphere (Liu et al., 2009, 2010a) and the somewhat lower OCS partial pressure in ambient air compared to that used in their experimental setup. Also, at steady state, adsorption should have little influence on the soil–air OCS exchange rate, unless heterogeneous (surface) reaction occurs and continuously removes OCS from the adsorbed phase (Liu et al., 2010a). In the following we will neglect adsorption of OCS on solid surfaces but we recognise that this assumption might be an over-simplification.

## A new mechanistic framework to predict OCS fluxes from soils

J. Ogée et al.

[Title Page](#)

[Abstract](#)

[Introduction](#)

[Conclusions](#)

[References](#)

[Tables](#)

[Figures](#)

◀

▶

◀

▶

[Back](#)

[Close](#)

[Full Screen / Esc](#)

[Printer-friendly Version](#)

[Interactive Discussion](#)



## 2.2 Mass balance equation

The transport of OCS through the soil matrix occurs by either pressure-driven (advective-dispersive) or concentration-driven (diffusive) fluxes. Carbonyl sulphide can also be destroyed or emitted, owing to abiotic and/or biotic processes. The general mass balance equation for OCS in a small soil volume can then be written:

$$\frac{\partial \varepsilon_{\text{tot}} C}{\partial t} = -\nabla F_{\text{diff}} - \nabla F_{\text{adv}} + P - S, \quad (1)$$

where  $\varepsilon_{\text{tot}} = \varepsilon_a + \theta B + \rho_b (K_{\text{sg}} + B K_{\text{sw}})$  ( $\text{m}^3 \text{air m}^{-3}$  soil) is total OCS soil porosity,  $F_{\text{diff}}$  ( $\text{mol m}^{-2} \text{s}^{-1}$ ) represents the diffusional flux of OCS through the soil matrix,  $F_{\text{adv}}$  ( $\text{mol m}^{-2} \text{s}^{-1}$ ) is the advective flux of OCS,  $P$  ( $\text{mol m}^{-3} \text{s}^{-1}$ ) the OCS production rate and  $S$  ( $\text{mol m}^{-3} \text{s}^{-1}$ ) the OCS consumption rate and  $\nabla = \partial/\partial x + \partial/\partial y + \partial/\partial z$  denotes the differential operator, i.e., the spatial gradient in all three directions  $x$ ,  $y$  and  $z$ .

If the soil is horizontally homogeneous (that is, the soil properties are independent of  $x$  and  $y$ ) and the soil lateral dimensions are much larger than its total depth (minimal edge effects), the OCS concentration is only a function of soil depth  $z$  and time  $t$  and Eq. (1) simplifies to:

$$\frac{\partial \varepsilon_{\text{tot}} C}{\partial t} = -\frac{\partial F_{\text{diff}}}{\partial z} - \frac{\partial F_{\text{adv}}}{\partial z} + P - S, \quad (2)$$

### 2.3 Diffusive fluxes

Diffusion in the gas phase is commonly described by Fick's first law (Bird et al., 2002; Scanlon et al., 2002):

$$F_{\text{diff, a}} = -D_{\text{eff, a}} \frac{\partial C}{\partial z}, \quad (3)$$

where  $F_{\text{diff, a}}$  ( $\text{mol m}^{-2} \text{soils}^{-1}$ ) is the diffusive flux of gaseous OCS and  $D_{\text{eff, a}}$  ( $\text{m}^3 \text{air m}^{-1} \text{soils}^{-1}$ ) is the effective diffusivity of gaseous OCS through the soil matrix.

[Title Page](#)

[Abstract](#)

[Introduction](#)

[Conclusions](#)

[References](#)

[Tables](#)

[Figures](#)

[◀](#)

[▶](#)

[◀](#)

[▶](#)

[Back](#)

[Close](#)

[Full Screen / Esc](#)

[Printer-friendly Version](#)

[Interactive Discussion](#)



## A new mechanistic framework to predict OCS fluxes from soils

J. Ogée et al.

[Title Page](#)

[Abstract](#)

[Introduction](#)

[Conclusions](#)

[References](#)

[Tables](#)

[Figures](#)

[◀](#)

[▶](#)

[◀](#)

[▶](#)

[Back](#)

[Close](#)

[Full Screen / Esc](#)

[Printer-friendly Version](#)

[Interactive Discussion](#)



The latter is commonly expressed relative to the binary diffusivity of OCS in free air  $D_{0,a}$  ( $\text{m}^2 \text{air s}^{-1}$ ):  $D_{\text{eff},a}/D_{0,a} = \tau_a \varepsilon_a$  where  $\tau_a$  is the so-called air tortuosity factor that accounts for the tortuosity of the air-filled pores, as well as their constrictivity and water-induced disconnectivity (e.g., Moldrup et al., 2003). The air-filled porosity ( $\varepsilon_a$ )

5 appears in this equation to account for the reduced cross-sectional area in the soil matrix relative to free air, although the effective porosity for diffusion could be smaller if the soil contains small pores that do not contribute to the overall transport such as dead end or blind pores. Expressions for  $\tau_a$  differ depending on whether the soil is repacked or undisturbed (Moldrup et al., 2003). For undisturbed soils the most com-

10 monly used equations are those of Penman (1940;  $\tau_a = 0.66$ , hereafter referenced as Pen40) and Millington and Quirk (1961;  $\tau_a = \varepsilon_a^{7/3}/\varphi^2$ , where  $\varphi$  is total soil porosity, hereafter referred to as MQ61). For repacked soils, equations proposed by Moldrup

et al. (2003;  $\tau_a = \varepsilon_a^{3/2}/\varphi$ , hereafter referred as Mol03) are preferred. For undisturbed soils with high porosity such as volcanic ash, the expression proposed by Moldrup

15 et al. (2003;  $\tau_a = \varepsilon_a^{1+3/b}/\varphi^{3/b}$ , where  $b$  is the pore-size distribution parameter) seems a better predictor (Moldrup et al., 2003). Recently a new density-corrected expression for undisturbed soils has also been proposed by Camindu Deepagoda et al. (2011;  $\tau_a = [0.2(\varepsilon_a/\varphi)^2 + 0.004]/\varphi$ ) that seems to be superior to previous formulations and has the advantage of not requiring knowledge of the pore-size distribution parameter  $b$ .

20 Diffusion in the liquid phase is described in a similar fashion to the gas phase (Olesen et al., 2001):

$$F_{\text{diff},l} = -D_{\text{eff},l} \frac{\partial C_l}{\partial z} = D_{\text{eff},l} \left\{ B \frac{\partial C}{\partial z} + C \frac{dB}{dT} \frac{\partial T}{\partial z} \right\}, \quad (4)$$

where  $F_{\text{diff},l}$  ( $\text{mol m}^{-2} \text{soil s}^{-1}$ ) is the diffusive flux of dissolved OCS in soil water and

25  $D_{\text{eff},l}$  ( $\text{m}^3 \text{water m}^{-1} \text{soil s}^{-1}$ ) is the effective diffusivity of dissolved OCS through the soil matrix. As for gaseous diffusion  $D_{\text{eff},l}$  is commonly expressed relative to the binary

diffusivity of OCS in free water  $D_{0,I}$  ( $\text{m}^2 \text{ waters}^{-1}$ ):  $D_{\text{eff},I}/D_{0,I} = \tau_I \theta$  where  $\tau_I$  is the tortuosity factor for solute diffusion. Commonly used expressions for  $\tau_I$  are those proposed by Penman (1940;  $\tau_I = 0.66$ ), Millington and Quirk (1961;  $\tau_I = \theta^{7/3}/\varphi^2$ ) and Moldrup et al. (2003;  $\tau_I = \theta^{b/3}/\varphi^{b/3-1}$ ).

5 Diffusion of OCS in the adsorbed phase can also theoretically occur and can be described in a similar fashion to other trace gases (e.g., see Choi et al., 2001 for ozone). However we will neglect such a diffusion flux in the adsorbed phase because it is expected to be orders of magnitude smaller than in the two other phases. Also the binary diffusivity of any trace gas is several orders of magnitude higher in the air than 10 it is for its dissolved counterpart in liquid water so that, in unsaturated (oxic) soils,  $F_{\text{diff}} = F_{\text{diff},a} + F_{\text{diff},I}$  is dominated by the gas-phase OCS diffusion flux  $F_{\text{diff},a}$ . The role of  $F_{\text{diff},I}$  in the OCS transport equations becomes significant only when the soil is water-logged.

15 The binary diffusivity  $D_{0,a}$  depends on pressure and temperature and is assumed here to follow the Chapman–Enskog theory for ideal gases (i.e., Bird et al., 2002):  $D_{0,a}(T, p) = D_{0,a}(T_0, p_0)(T/T_0)^{1.5}(p_0/p)$ . A value for  $D_{0,a}$  ( $25^\circ\text{C}$ , 1 atm) of  $1.27 \times 10^{-5} \text{ m}^2 \text{ s}^{-1}$  is used and based on the value for the diffusivity of water vapour in air at  $25^\circ\text{C}$  ( $2.54 \times 10^{-5} \text{ m}^2 \text{ s}^{-1}$ , see Massman (1998)) and the  $\text{CO}_2/\text{OCS}$  diffusivity ratio of  $2.0 \pm 0.2$  derived from the Chapman–Enskog theory and the difference in molar 20 masses of OCS and  $\text{CO}_2$  (Seibt et al., 2010). The binary diffusivity  $D_{0,I}$  also depends on temperature (Ulshöfer et al., 1996). Because the Stokes–Einstein equation only applies to spherical suspended particles we prefered to use an empirical equation that works well for both the self-diffusivity of water and the diffusivity of dissolved  $\text{CO}_2$  in liquid 25 water (Zeebe, 2011):  $D_{0,I}(T) = D_{0,I}(T_0)(T/T_0 - 1)^2$ , with  $D_{0,I}(25^\circ\text{C}) = 1.94 \times 10^{-9} \text{ m}^2 \text{ s}^{-1}$  (Ulshöfer et al., 1996) and  $T_0 = 216\text{K}$ . This value of  $T_0$  was chosen to be intermediate between the value used for water ( $215.05\text{K}$ ) and dissolved  $\text{CO}_2$  ( $217.2\text{K}$ ) (Zeebe, 2011) and results in a temperature dependency of  $D_{0,I}$  for OCS in water in very good agreement with relationships found in other studies (Fig. 1b).

Title Page

Abstract

Introduction

Conclusions

References

Tables

Figures

◀

▶

◀

▶

Back

Close

Full Screen / Esc

Printer-friendly Version

Interactive Discussion



## 2.4 Advectional fluxes

Advection of OCS can occur in both the liquid and gas phases when the carrier fluid (water or air) moves relative to the soil matrix:

$$F_{\text{adv},l} = q_l C_l = q_l BC, \quad (5a)$$

<sup>5</sup>  $F_{\text{adv},a} = q_a C, \quad (5b)$

where  $q_l$  ( $\text{m s}^{-1}$ ) and  $q_a$  ( $\text{m s}^{-1}$ ) are the velocity fields for liquid water and air respectively. If the flow in the porous soil is laminar these velocity fields are given by Darcy's law (Massman et al., 1997; Scanlon et al., 2002):

$$q_l = -\frac{k_l}{\mu_l} \frac{\partial \Psi_l}{\partial z} = -K_l \left( \frac{\partial h_l}{\partial z} + 1 \right), \quad (6a)$$

<sup>10</sup>  $q_a = -\frac{k_a}{\mu_a} \left( \frac{\partial p_a}{\partial z} + \rho_a g \right). \quad (6b)$

In Eqs. (6a) and (6b)  $k_l$  and  $k_a$  ( $\text{m}^2$ ) denote soil permeabilities for liquid water and air respectively,  $\mu_l$  and  $\mu_a$  ( $\text{kg m}^{-1} \text{s}^{-1}$ ) are water and air dynamic viscosities,  $\Psi_l = \rho_l g(h_l + z)$  is total soil water potential (Pa),  $\rho_l$  is water density ( $1000 \text{ kg m}^{-3}$ ),  $g$  is gravitational acceleration ( $9.81 \text{ m s}^{-2}$ ),  $\rho_a$  is air density (ca.  $1.2 \text{ kg m}^{-3}$ ) and  $p_a$  (Pa) is air pressure. We

<sup>15</sup> also defined the soil hydraulic conductivity  $K_l$  ( $\text{m s}^{-1}$ ):  $K_l = k_l \rho_l g / \mu_l$ . In practice  $p_a$  can be expressed as the sum of the hydrostatic pressure ( $p_{ah} = -\rho_a g z$ ) and a fluctuating (non-hydrostatic) part:  $p_a = -\rho_a g z + p'_a$  so that Eq. (6b) can be replaced by:

$$q_a = -\frac{k_a}{\mu_a} \frac{\partial p'_a}{\partial z}. \quad (6c)$$

From Eq. (6c) we can see that advection in the gas phase can result from pressure fluctuations, caused by, e.g., venting the soil surface (according to Bernouilli's equation)

BGD

12, 15687–15736, 2015

A new mechanistic framework to predict OCS fluxes from soils

J. Ogée et al.

[Title Page](#)

[Abstract](#)

[Introduction](#)

[Conclusions](#)

[References](#)

[Tables](#)

[Figures](#)

◀

▶

◀

▶

[Back](#)

[Close](#)

[Full Screen / Esc](#)

[Printer-friendly Version](#)

[Interactive Discussion](#)



or turbulence above the soil surface. Typical air pressure fluctuations are of the order of 10 Pa (Maier et al., 2012; Massman et al., 1997). Pressure fluctuations can also result from non-hydrostatic density fluctuations caused by a change in the air composition with gas species of different molar mass as air or by temperature gradients, but the resulting flux is significant only in highly permeable (i.e. fractured) soils.

When averaged over a long enough timescale ( $> 1$  h) the advective flux starts to become negligible compared to the diffusive flux (e.g., Massman et al., 1997). Integration timescales of a few minutes were already assumed to allow liquid–vapour equilibration in Eq. (5a). In the following we will thus neglect advective fluxes in the OCS budget equation, keeping in mind that such an assumption is valid only for time scales of about 1 h or longer.

Even when advective fluxes are negligible, advection through porous media generates a diffusive-like flux called mechanical dispersion that reflects the fact that not everything in the porous medium travels at the average water or gas flow speed. Some paths are faster, some slower, some longer and some shorter, leading to a net spreading of the gas or solute plume that looks very much like a diffusive behaviour. Since mechanical dispersion depends on the flow, it is expected to increase with increasing flow speed and is usually expressed as:

$$F_{\text{disp},l} = -D_{\text{disp},l} \frac{\partial C_l}{\partial z} = -\alpha_l |q_l| \frac{\partial BC}{\partial z}, \quad (7a)$$

$$F_{\text{disp},a} = -D_{\text{disp},a} \frac{\partial C}{\partial z} = -\alpha_a |q_a| \frac{\partial C}{\partial z}, \quad (7b)$$

where  $\alpha_l$  (m) and  $\alpha_a$  (m) are the longitudinal dynamic dispersivity of liquid water and air flow respectively and  $D_{\text{disp},l}$  ( $\text{m}^2 \text{s}^{-1}$ ) and  $D_{\text{disp},a}$  ( $\text{m}^2 \text{s}^{-1}$ ) are the corresponding dispersive diffusivities. Transverse dispersion (i.e. in a plane perpendicular to the flow) can also occur but will be neglected here.

In practice, because of advective-dispersive fluxes, we must know the liquid water and air velocity fields  $q_l$  and  $q_a$  in order to solve the trace gas OCS mass budget

## A new mechanistic framework to predict OCS fluxes from soils

J. Ogée et al.

[Title Page](#)

[Abstract](#)

[Introduction](#)

[Conclusions](#)

[References](#)

[Tables](#)

[Figures](#)

[|◀](#)

[▶|](#)

[◀](#)

[▶](#)

[Back](#)

[Close](#)

[Full Screen / Esc](#)

[Printer-friendly Version](#)

[Interactive Discussion](#)



Eq. (2). This requires solving the total mass balance equations for liquid water and air separately. However, except during rain infiltration and immediate redistribution  $q_l$  rarely exceeds a few mm per day while the drift velocity  $F_{\text{diff, a}}/C$  is typically of the order of a few mm per minute. For this reason, advection fluxes are generally neglected in soil gas transport models. Dispersive fluxes can still be accounted for as a correction factor to true diffusion, provided we have parameterisations of the dispersion diffusivities that are independent of the advective flux (e.g., expressions for  $D_{\text{disp, a}}$  independent of  $q_a$ ). For example Maier et al. (2012) proposed expressions of  $D_{\text{disp, a}}/D_{0,a}$  that rely on the air-filled porosity ( $\varepsilon_a$ ) and permeability ( $\mu_a$ ) of the soil and the degree of turbulence above the soil surface (characterised by the friction velocity  $u_*$ ).

## 2.5 Consumption and production rates

The processes of consumption or production of OCS in a soil are not fully understood. Carbonyl sulphide can be consumed through hydrolysis in the bulk soil water at an un-catalysed rate  $k_{\text{uncat}}$  ( $\text{s}^{-1}$ ) that depends mostly on temperature  $T$  and pH (Elliott et al., 1989). In the following we will use the expression proposed by Elliott et al. (1989) because it covers the widest range of temperature and pH:

$$k_{\text{uncat}} = 2.15 \times 10^{-5} \exp \left( -10450 \left( \frac{1}{T} - \frac{1}{298} \right) \right) + 12.7 \times 10^{-pK_w + pH} \exp \left( -6040 \left( \frac{1}{T} - \frac{1}{298} \right) \right), \quad (8)$$

where  $pK_w$  is the dissociation constant of water. Other expressions are available in the literature and compared to Eq. 8 for both temperature (Fig. 1c) and pH (Fig. 2a) responses. Using Eq. 8 the uncatalysed OCS uptake rate is then computed as  $S_{\text{uncat}} = k_{\text{uncat}} B \theta C$ .

This uncatalysed rate is rather small and cannot explain the large OCS uptake rates observed in oxic soils (Kesselmeier et al., 1999; J. Liu et al., 2010; Van Diest and

BGD

12, 15687–15736, 2015

A new mechanistic framework to predict OCS fluxes from soils

J. Ogée et al.

<a href="#">Title Page</a>	
<a href="#">Abstract</a>	<a href="#">Introduction</a>
<a href="#">Conclusions</a>	<a href="#">References</a>
<a href="#">Tables</a>	<a href="#">Figures</a>
<a href="#">◀</a>	<a href="#">▶</a>
<a href="#">◀</a>	<a href="#">▶</a>
<a href="#">Back</a>	<a href="#">Close</a>
<a href="#">Full Screen / Esc</a>	
<a href="#">Printer-friendly Version</a>	
<a href="#">Interactive Discussion</a>	



Kesselmeier, 2008). The main consumption of OCS is thought to be enzymatic and governed by soil micro-organisms' CA activity (Kesselmeier et al., 1999; J. Liu et al., 2010; Van Diest and Kesselmeier, 2008). We will assume that such a catalysed reaction by CA-containing organisms can be described by Michaelis–Menten kinetics, as was observed for OCS in several marine algae species (Bleizinger et al., 2000; Protoschill-Krebs et al., 1995) and one flour beetle (Haritos and Dojchinov, 2005). Because of the low levels of OCS concentration in ambient air (500 ppt) and the comparatively high values of the Michaelis–Menten coefficient for OCS ( $K_m$ , see Ogawa et al., 2013; Protoschill-Krebs et al., 1995, 1996) the catalysed uptake rate  $S_{\text{cat}}$  ( $\text{s}^{-1}$ ) can be approximated:

$$S_{\text{cat}} = \theta k_{\text{cat}} [\text{CA}] \frac{BC}{K_m + BC} \approx \frac{k_{\text{cat}}}{K_m} [\text{CA}] B \theta C, \quad (9)$$

where  $k_{\text{cat}}$  ( $\text{s}^{-1}$ ) and  $K_m$  ( $\text{mol m}^{-3}$ ) are the turnover rate and the Michaelis–Menten constant of the enzymatic reaction, respectively and  $[\text{CA}]$  ( $\text{mol m}^{-3}$ ) is the total CA concentration in soil water. We recognise that Eq. (9) is an over-simplification of the reality in the sense that  $k_{\text{cat}}$  and  $K_m$  are not true kinetic parameters but rather spatially-averaged, organism-level parameters. Also Eq. (9) neglects the competition for CA by  $\text{CO}_2$  molecules and the co-limination of the uptake by diffusional constraints. Given the Michaelis–Menten constant of CA for  $\text{CO}_2$  (of the order of 3 mM at 25 °C and pH 8–9) and the range of  $\text{CO}_2$  mixing ratios encountered in soil surfaces (300–10 000 ppm or 0.01–0.3 mM at 25 °C and 1 atm) we can easily show that the competition with  $\text{CO}_2$  is negligible. Using typical values of bacterial population size and of transfer conductance across lipid bilayers (Evans et al., 2009) we can also show that the limitation of OCS uptake by diffusion across cell membranes is negligible.

As found for any enzymatic reaction  $k_{\text{cat}}$  and  $K_m$  depend on temperature and internal pH ( $\text{pH}_{\text{in}}$ ). In the following we will assume that the ratio  $k_{\text{cat}}/K_m$  has a temperature

Title Page

Abstract

Introduction

Conclusions

References

Tables

Figures

◀

▶

◀

▶

Back

Close

Full Screen / Esc

Printer-friendly Version

Interactive Discussion



dependency that can be approximated as:

$$\frac{k_{\text{cat}}}{K_m} \propto x_{\text{CA}}(T) = \frac{\exp(-E_a/RT)}{1 + \exp(-E_d/RT + S_d/R)}, \quad (10a)$$

where  $E_a$ ,  $E_d$  and  $S_d$  are thermodynamic parameters. In the following we will take  $E_a = 40 \text{ kJ mol}^{-1}$ ,  $E_d = 200 \text{ kJ mol}^{-1}$  and  $S_d = 660 \text{ J mol}^{-1} \text{ K}^{-1}$ , that leads to a temperature optima  $T_{\text{opt,CA}} = 25^\circ\text{C}$  and reproduces well the temperature response of  $\beta$ -CA

5 found on maize leaf extracts observed in the range 0–17°C by Burnell et al. (1988) (Fig. 1d). To our knowledge this is the only study that reports the temperature response of  $\beta$ -CA, the dominant CA class expected in soils (Smith et al., 1999). Interestingly our parameterisation of  $x_{\text{CA}}(T)$ , based on direct measurements on  $\beta$ -CA from Burnell  
10 et al. (1988), is very different from the one used by Sun et al. (2015), especially at temperatures above 20°C (Fig. 1d). The value for  $K_m$  (39  $\mu\text{M}$  at 20°C and pH 8.2) was taken from Protoschill-Krebs et al. (1996) and  $k_{\text{cat}}$  was estimated at  $93 \text{ s}^{-1}$  at the same temperature and pH from a re-analysis of the same dataset, leading to a  $k_{\text{cat}}/K_m$  value  
15 of  $2.39 \text{ s}^{-1} \mu\text{M}^{-1}$ . To our knowledge this is the only study that reports  $k_{\text{cat}}$  and  $K_m$  values for OCS in  $\beta$ -CA.

The pH response of CA activity for OCS hydrolysis was described by a monotonic decrease function towards more acidic  $\text{pH}_{\text{in}}$ , as observed in plant  $\beta$ -CA for both OCS (Protoschill-Krebs et al., 1996) and  $\text{CO}_2$  (Rowlett et al., 2002). In the following we will use the expression proposed by Rowlett et al. (2002) for  $\text{CO}_2$ :

$$\frac{k_{\text{cat}}}{K_m} \propto y_{\text{CA}}(\text{pH}_{\text{in}}) = \frac{1}{1 + 10^{-\text{pH}_{\text{in}} + pK_{\text{CA}}}}, \quad (10b)$$

20 A value of  $pK_{\text{CA}} = 7.2$  was used that corresponds to the CA response of the wild-type *Arabidopsis thaliana* (Rowlett et al., 2002). The shape of the function  $y_{\text{CA}}$  is shown in Fig. 2b.

25 The breaking of water film continuity that occurs at low soil water content leads to a reduction in microbial activity owing to the spatial separation of the microbes and their

[Title Page](#)

[Abstract](#)

[Introduction](#)

[Conclusions](#)

[References](#)

[Tables](#)

[Figures](#)

[◀](#)

[▶](#)

[◀](#)

[▶](#)

[Back](#)

[Close](#)

[Full Screen / Esc](#)

[Printer-friendly Version](#)

[Interactive Discussion](#)



<a href="#">Title Page</a>	
<a href="#">Abstract</a>	<a href="#">Introduction</a>
<a href="#">Conclusions</a>	<a href="#">References</a>
<a href="#">Tables</a>	<a href="#">Figures</a>
<a href="#">◀</a>	<a href="#">▶</a>
<a href="#">◀</a>	<a href="#">▶</a>
<a href="#">Back</a>	<a href="#">Close</a>
<a href="#">Full Screen / Esc</a>	
<a href="#">Printer-friendly Version</a>	
<a href="#">Interactive Discussion</a>	



respiratory substrates (Manzoni and Katul, 2014). In our case soil water discontinuity should not affect OCS supply as gaseous OCS should be equally available in all soil pores. On the other hand different organisms may have different  $k_{\text{cat}}/K_m$  values so that the spatially-averaged  $k_{\text{cat}}/K_m$  could vary with drought-induced changes in microbial diversity. However our knowledge of how  $k_{\text{cat}}/K_m$  for OCS varies amongst different life forms is too scarce to know if it should increase or decrease during drought stress. We will therefore assume that soil water discontinuity does not affect  $k_{\text{cat}}/K_m$  directly. CA concentration ([CA]) could also vary during drought stress, although it is not clear in which direction. During water stress microbial activity such as respiration or growth is usually reduced, but slow growth rates and heat stress have been shown to cause an up-regulation of CA-gene expression in *Escherichia coli* (Merlin et al., 2003), probably because of a need of bicarbonate for lipid synthesis. For this study we thus make the simplifying assumption that CA concentration does not vary with soil water content. The catalysed OCS uptake rate  $S_{\text{cat}}$  is then simply proportional to soil water content (Eq. 9).

Destruction of OCS can also occur in the solid phase and was observed on pure mineral oxides with high basicity (Liu et al., 2008, 2009; 2010a). However, such catalytic reaction should be significant only in very dry soils (with only a few molecular layers of water) and in the absence of other competitive adsorbents such as  $\text{CO}_2$  (Liu et al., 2008, 2010b) and is therefore neglected in our model. The total soil OCS uptake rate is thus computed as  $S = kB\theta C$  with:

$$k = k_{\text{uncat}}(T, \text{pH}) + \frac{x_{\text{CA}}(T)}{x_{\text{CA}}(20^\circ\text{C})} \frac{y_{\text{CA}}(\text{pH}_{\text{in}})}{y_{\text{CA}}(8.2)} 2390[\text{CA}]. \quad (11)$$

Following common practice in the  $\text{CO}_2$  literature we will also express  $k$  with respect to the uncatalysed rate at  $25^\circ\text{C}$  and pH 4.5, i.e.,  $k = f_{\text{CA}} k_{\text{uncat}}(25^\circ\text{C}, \text{pH} = 4.5)$ , where  $f_{\text{CA}}$  is the so-called soil CA enhancement factor. We can see from Eq. (11) that  $f_{\text{CA}}$  is not an intrinsic property of the soil and will vary with temperature, and pH, even at constant CA concentration.

In some situations the OCS uptake rates can be overridden by OCS production. This is the case when soil temperature rises above 25 °C (Whelan and Rhew, 2015) or soil redox potential falls below –100 mV (Devai and Delaune, 1995). Light has also been proposed as an important trigger of OCS production, assuming photoproduction processes similar to those observed in ocean waters can occur (Whelan and Rhew, 2015). However the literature and data on this possible mechanism is still too scarce and not quantitative enough to be accounted for in our model.

The soil redox potential ( $E_h$ ) is a very dynamic variable that is not easily measured in the field, especially in unsaturated soils (e.g., van Bochove et al., 2002). Although  $E_h$  and pH are linked, their relationship is not unique and depends on the set of oxydants and reductants present in the soil solution (e.g., Delaune and Reddy, 2005). Also the soil redox potential is probably a more direct trigger for OCS production as it defines when sulfate ions start to become limiting for the plants or the soil microbes (Husson, 2012). For this study we thus consider that  $E_h$  is the primary driver of OCS production, independently of pH:

$$P = P_{\text{ref}} y_P(E_h) Q_{10}^{(T - T_{\text{ref}})/10}, \quad (12a)$$

where  $P_{\text{ref}}$  ( $\text{mol m}^{-3} \text{ s}^{-1}$ ) is the production rate at temperature  $T_{\text{ref}}$  (K) and low  $E_h$  (typically –200 mV) and  $Q_{10}$  is the multiplicative factor of the production rate for a 10 °C temperature rise. According to results from Devai and DeLaune (1995), the function  $y_P(E_h)$  may be expressed as:

$$y_P(E_h) = \frac{1}{1 + \exp((E_h - 100 \text{ mV})/20 \text{ mV})}. \quad (12b)$$

Because soil OCS emission, when observed in oxic soils, usually occurs at temperature around 25 °C or higher, we will set  $T_{\text{ref}} = 25$  °C and thus  $P_{\text{ref}} = P_{25}$ .

## A new mechanistic framework to predict OCS fluxes from soils

J. Ogée et al.

[Title Page](#)

[Abstract](#)

[Introduction](#)

[Conclusions](#)

[References](#)

[Tables](#)

[Figures](#)

[◀](#)

[▶](#)

[◀](#)

[▶](#)

[Back](#)

[Close](#)

[Full Screen / Esc](#)

[Printer-friendly Version](#)

[Interactive Discussion](#)



## 2.6 Steady-state solution

The one-dimensional mass balance equation (Eq. 2) can be re-written as:

$$\frac{\partial \varepsilon_t C}{\partial t} = \frac{\partial}{\partial z} \left\{ (D_{\text{disp}, a} + \alpha_a |q_a|) \frac{\partial C}{\partial z} + (D_{\text{disp}, l} + \alpha_l |q_l|) \frac{\partial BC}{\partial z} \right\} + P - kB\theta C, \quad (13)$$

Assuming steady-state conditions and isothermal and uniform conditions, this simplifies to:

$$D \frac{d^2 C}{dz^2} - kB\theta C = -P, \quad (14)$$

with:

$$D = D_{\text{disp}, a} + \alpha_a |q_a| + (D_{\text{disp}, l} + \alpha_l |q_l|)B, \quad (15)$$

Boundary conditions are  $C(z = 0) = C_a$ , the OCS concentration in the air above the soil column and  $dC/dz(z = z_{\max}) = 0$ , i.e., zero flux at the bottom of the soil column, located at depth  $z_{\max}$  (the case for laboratory measurements). With such boundary conditions, the solution of Eq. (14) is:

$$C(z) = z_1^2 P + (C_a - z_1^2 P) \frac{e^{-z/z_1} + \xi^2 e^{+z/z_1}}{1 + \xi^2}, \quad (16a)$$

with  $z_1^2 = D/kB\theta$  and  $\xi = e^{-z_{\max}/z_1}$ . This leads to an OCS efflux at the soil surface:

$$F = \sqrt{kB\theta D} \left( C_a - \frac{z_1^2 P}{D} \right) \frac{1 - \xi^2}{1 + \xi^2}, \quad (16b)$$

from which we can deduce the deposition velocity  $V_d = F/C_a$ .

[Title Page](#)

[Abstract](#)

[Introduction](#)

[Conclusions](#)

[References](#)

[Tables](#)

[Figures](#)

◀

▶

◀

▶

[Back](#)

[Close](#)

[Full Screen / Esc](#)

[Printer-friendly Version](#)

[Interactive Discussion](#)



For field datasets, the condition at the lower boundary should be modified to  $dC/dz(z \rightarrow \infty) = 0$  and the production rate  $P$  should be positive and uniform only over a certain depth  $z_P$  below the surface. In this case the steady-state solution becomes:

$$F = \sqrt{kB\theta D} \cdot \left( C_a - \frac{z_1^2 P}{D} (1 - \exp(-z_P/z_1)) \right), \quad (17)$$

We can verify that both equations give the same results if  $z_{\max} \rightarrow \infty$  and  $z_P \rightarrow \infty$ , and also that Eq. (17) leads to  $F \rightarrow -Pz_P$  when  $k \rightarrow 0$ .

## 2.7 Soil incubation datasets used for model validation

The steady-state OCS deposition model presented here (Eq. 16b) was evaluated against measurements performed on different soils in the laboratory. For this purpose we revisited the dataset presented in VanDiest and Kesselmeier (2008). Volumetric soil moisture content ( $\theta$ , in  $\text{cm}^3(\text{H}_2\text{O})\text{cm}^{-3}$ , soil) was converted from gravimetric soil water content data ( $M_{w, \text{soil}}$ , in  $\text{g}(\text{H}_2\text{O})\text{g}(\text{soil})^{-1}$ ) by means of the bulk density of the soil inside the chamber ( $\rho_b$ , in  $\text{g}\text{cm}^{-3}$ ):  $\theta = M_{w, \text{soil}}\rho_b/\rho_w$ , where  $\rho_w = 1 \text{ g}\text{cm}^{-3}$  is the density of liquid water. The soil bulk density was itself estimated from the maximum soil moisture content after saturation ( $\theta_{\max} = M_{w, \text{soil, max}}\rho_b/\rho_w$ ), assuming the latter corresponded to soil porosity ( $\varphi = 1 - \rho_b/2.66$ ), i.e., ( $\rho_b = 1/(M_{w, \text{soil, max}}/\rho_w + 1/2.66)$ ). Soil thickness ( $z_{\max}$ ) was further estimated using  $\rho_b$ , soil dry weight (200 g for the German soil, 80 g for the other soils) and soil surface area ( $165.1 \text{ cm}^2$ ) assuming soil density was uniform. Air porosity was calculated as:  $\varepsilon_a = \varphi - \theta$ .

[Title Page](#)[Abstract](#)[Introduction](#)[Conclusions](#)[References](#)[Tables](#)[Figures](#)[◀](#)[▶](#)[◀](#)[▶](#)[Back](#)[Close](#)[Full Screen / Esc](#)[Printer-friendly Version](#)[Interactive Discussion](#)

### 3 Results

#### 3.1 Sensitivity to diffusivity model

Given the large diversity of expressions for the air tortuosity factor ( $\tau_a$ ) used to compute the effective diffusivity of OCS through the soil matrix, we felt it important to perform a sensitivity analysis of the model to different formulations available in the literature for  $\tau_a$ . In Fig. 3 we show how the steady-state soil OCS deposition velocity model (Eq. 16b) responds to soil moisture or soil temperature for three different formulations of  $\tau_a$ : Pen40 ( $\tau_a = 0.66$ ), MQ61 ( $\tau_a = \varepsilon_a^{7/3}/\varphi^2$ ) and Mol03 ( $\tau_a = \varepsilon_a^{3/2}/\varphi$ ). We also indicate the optimal soil moisture ( $\theta_{opt}$ ) and temperature ( $T_{opt,Vd}$ ) for each formulation.

We found that the optimal temperature and the general shape of the response to temperature were not affected by the choice of the diffusivity model (Fig. 3, right panel). On the other hand the optimal soil moisture and the general shape of the response to soil moisture strongly depended on the choice made for  $\tau_a$  (Fig. 3, left panel). In particular the model of Penman (1940) gives a perfectly symmetric response to soil moisture with an optimal value at  $\theta_{opt} = \varphi/2$ , unlike other formulations:  $\theta_{opt} = 0.3\varphi/1.3$  for Millington and Quirk (1961) and  $\theta_{opt} = 2\varphi/7$  for Moldrup et al. (2003).

It is also noticeable on the right panel of Fig. 3 that the optimal temperature for  $V_d$  ( $T_{opt,Vd}$ ) is actually lower than the prescribed optimal temperature for the catalysed OCS hydrolysis rate ( $T_{opt,CA} = 25^\circ\text{C}$  in this case), even in the absence of an OCS source term. This is because  $T_{opt,Vd}$  integrates other temperature responses, from the total effective diffusivity ( $D$ ) and the OCS solubility ( $B$ ). Although these variables do not exhibit a temperature optimum, their temperature responses affect the overall value of  $T_{opt,Vd}$ . It can be shown analytically that this leads to  $T_{opt,Vd} < T_{opt,CA}$ .

#### 3.2 Sensitivity to soil depth

Laboratory-based measurements of soil–air OCS fluxes are generally performed on small soil samples whose thickness are no more than a few centimetres. In contrast

BGD

12, 15687–15736, 2015

A new mechanistic framework to predict OCS fluxes from soils

J. Ogée et al.

<a href="#">Title Page</a>	
<a href="#">Abstract</a>	<a href="#">Introduction</a>
<a href="#">Conclusions</a>	<a href="#">References</a>
<a href="#">Tables</a>	<a href="#">Figures</a>
<a href="#">◀</a>	<a href="#">▶</a>
<a href="#">◀</a>	<a href="#">▶</a>
<a href="#">Back</a>	<a href="#">Close</a>
<a href="#">Full Screen / Esc</a>	
<a href="#">Printer-friendly Version</a>	
<a href="#">Interactive Discussion</a>	



## A new mechanistic framework to predict OCS fluxes from soils

J. Ogée et al.

[Title Page](#)

[Abstract](#)

[Introduction](#)

[Conclusions](#)

[References](#)

[Tables](#)

[Figures](#)

[◀](#)

[▶](#)

[◀](#)

[▶](#)

[Back](#)

[Close](#)

[Full Screen / Esc](#)

[Printer-friendly Version](#)

[Interactive Discussion](#)



flux measurements performed in the field account for the entire soil column beneath the chamber enclosure. In order to see whether results from laboratory measurements could be directly applied to field conditions we performed a sensitivity analysis of the model to soil thickness (Fig. 4). We found that the responses to both soil moisture and soil temperature were affected by maximum soil depth ( $z_{\max}$ ), at least when  $z_{\max}$  was below a few centimetres. Thin soils lead to lower maximum deposition rates but higher values of  $\theta_{\text{opt}}$  and  $T_{\text{opt,Vd}}$ . In Fig. 4 this is true mostly for  $z_{\max} = 1 \text{ cm}$ , and as soon as  $z_{\max}$  reaches values above or equal to  $3 \text{ cm}$ , the response curve becomes almost indistinguishable from that obtained with  $z_{\max} = 100 \text{ cm}$ .

However this threshold on  $z_{\max}$  also depends on soil CA activity. Results shown in Fig. 4 were obtained with an enhancement factor for OCS hydrolysis  $f_{\text{CA}}$  of 30 000. A smaller enhancement factor would have led to a deeper transition zone (e.g. about  $10 \text{ cm}$  with  $f_{\text{CA}}$  of 1000). This is because in Eq. (16b), the steady-state model of OCS deposition is proportional to  $\tanh(z_{\max}/z_1)$ . Given the shape of the hyperbolic tangent function, we expect our steady-state OCS deposition velocity model to become insensitive to  $z_{\max}$  as soon as  $z_{\max}/z_1 \geq 2$ . With  $z_1 = \sqrt{D/kB\theta}$  and because  $k$  is proportional to  $f_{\text{CA}}$  we can see that this condition on  $z_{\max}/z_1$  will depend on  $f_{\text{CA}}$ . At  $f_{\text{CA}} = 1000$ , we have  $z_1(\theta_{\text{opt}}) \sim 5 \text{ cm}$  while at  $f_{\text{CA}} = 10 000$  we have  $z_1(\theta_{\text{opt}}) \sim 1.5 \text{ cm}$ .

This response to soil depth was already observed by Kesselmeier et al. (1999) who reported measurements of OCS deposition velocity that increased linearly with the quantity of soil in their soil chamber enclosure up to  $200 \text{ g}$  of soil and then reached a plateau at around  $400 \text{ g}$ . Because their soil samples were evenly spread inside the soil chamber, an increase in the quantity of soil directly translates into an increase in soil thickness. Using an enhancement factor  $f_{\text{CA}}$  of 27 000 we were able to reproduce their saturation curve with soil weight using our steady-state model (Fig. 5). A lower  $f_{\text{CA}}$  value would have reduced the curvature of the model but would have also lowered the maximum  $V_d$  (not shown, but see Fig. 6). A value for  $f_{\text{CA}}$  of 27 000 was the best compromise to match the observed saturation curve. Because different soil weights were measured at different times with new soil material each time, it is possible that

they would correspond to slightly different  $f_{CA}$  values and this could explain the slight mismatch between the model and the observations.

### 3.3 Sensitivity to soil CA activity and OCS emission rates

Two model parameters are not well constrained: these are the CA concentration (or conversely the CA enhancement factor  $f_{CA}$ ) and the OCS production rate at 25 °C ( $P_{25}$ ). A sensitivity analysis of our steady-state OCS deposition model to these two parameters is shown in Figs. 6 and 7. Both parameters affect the maximum deposition rates but in opposite direction, with high  $f_{CA}$  values leading to higher  $V_d$  and high  $P_{25}$  values leading to lower  $V_d$ . This was expected from Eq. (16b) as  $V_d$  is proportional to  $\sqrt{f_{CA}}$  and is linearly and negatively related to  $P_{25}$ .

Interestingly, the optimal soil moisture is not modified by changes in  $f_{CA}$  (Fig. 6, left panel) and only slightly by  $P_{25}$  (Fig. 7, left panel). This means that, provided that  $z_{max}$  is known precisely (or larger than  $2z_1$ , see Sect. 3.2), the overall shape of the response to soil moisture (as typically measured during a drying cycle) and the exact value of  $\theta_{opt}$  are indicative solely of the diffusivity model to be used (Fig. 3). This result is important and should help us to, at least, decide whether the Pen40 formulation for  $\tau_a$  must be used instead of a more asymmetrical one (the Mol03 and MQ61 formulations are harder to distinguish, see Fig. 3).

The value of  $T_{opt,V_d}$  is also insensitive to changes in  $f_{CA}$  (Fig. 6, right panel) but diminishes when  $P_{25}$  increases (Fig. 7, right panel). This means that very low optimal temperature values  $T_{opt,V_d}$  (i.e. unusually low compared to expected values for enzymatic activities and  $T_{opt,CA}$ ) should be indicative of an OCS emission term, even if the values of  $V_d$  remain positive (i.e. the soil acts as a sink) in the temperature range explored. Of course at higher temperature, and because in our model the OCS source term responds exponentially with temperature ( $Q_{10}$  response) while  $k$  exhibits an optimal temperature ( $T_{opt,CA}$ ), the  $V_d$  should reach negative values if the value of  $P_{25}$  is large and  $f_{CA}$  is low. In some extreme cases where  $P_{25}$  fully dominates over  $f_{CA}$ , our model could even predict OCS fluxes close to zero at temperatures below ~10 °C that

BGD

12, 15687–15736, 2015

A new mechanistic framework to predict OCS fluxes from soils

J. Ogée et al.

[Title Page](#)

[Abstract](#)

[Introduction](#)

[Conclusions](#)

[References](#)

[Tables](#)

[Figures](#)

◀

▶

◀

▶

[Back](#)

[Close](#)

[Full Screen / Esc](#)

[Printer-friendly Version](#)

[Interactive Discussion](#)



would increase exponentially at warmer temperatures, as it has been observed in some agricultural soils (J. Liu et al., 2010; Maseyk et al., 2014; Whelan and Rhew, 2015).

BGD

12, 15687–15736, 2015

A new mechanistic framework to predict OCS fluxes from soils

J. Ogée et al.

[Title Page](#)

[Abstract](#)

[Introduction](#)

[Conclusions](#)

[References](#)

[Tables](#)

[Figures](#)

[◀](#)

[▶](#)

[◀](#)

[▶](#)

[Back](#)

[Close](#)

[Full Screen / Esc](#)

[Printer-friendly Version](#)

[Interactive Discussion](#)



et al. (2003), was able to reproduce most observed response curves to soil drying (Figs. 9–12, left and middle panels). The model was also able to reproduce, within the measurement uncertainties, the temperature dependency of  $V_d$  at a soil moisture level of  $0.12 \text{ cm}^3 \text{ cm}^{-3}$  (far right panels in Figs. 9–12).

## 5 4 Discussion

### 4.1 Can the proposed model explain observations realistically?

Many studies have clearly demonstrated that soil moisture strongly modulates OCS uptake by soils, with an optimal soil moisture content usually around 12 % of soil weight (Kesselmeier et al., 1999; J. Liu et al., 2010; Van Diest and Kesselmeier, 2008). As

10 noted in some of these studies, such a bell-shape response is indicative of reactional and diffusional limitations at low and high soil moisture contents, respectively. Using our steady-state formulation for shallow soils (Eq. 12b) we were able to reproduce almost exactly the soil moisture response observed experimentally (Fig. 9–12). We also found that the observed asymmetric response to soil moisture was best captured by the soil 15 diffusivity model of Moldrup et al. (2003) or Millington and Quirk (1961) and showed that the optimum soil moisture could be related to soil porosity:  $\theta_{\text{opt}} = 0.3\varphi/1.3$  for MQ61 and  $\theta_{\text{opt}} = 2\varphi/7$  for Mol03. Using our model we were also able to explain the response of OCS uptake to soil weight (i.e. soil thickness) observed by Kesselmeier et al. (1999) (Fig. 5).

20 We also tested our model against observations of the temperature response of  $V_d$ . Empirical studies showed that, for a given soil, the maximum OCS uptake rate was modulated by incubation temperature, with an optimal temperature ranging from 15 to 35 °C (Kesselmeier et al., 1999; J. Liu et al., 2010; Van Diest and Kesselmeier, 2008). This temperature response was interpreted as an enzymatically catalysed process, 25 governed by soil micro-organisms' CA activity (Kesselmeier et al., 1999; J. Liu et al., 2010; Van Diest and Kesselmeier, 2008). To reproduce this response of  $V_d$  to incubation

<a href="#">Title Page</a>	
<a href="#">Abstract</a>	<a href="#">Introduction</a>
<a href="#">Conclusions</a>	<a href="#">References</a>
<a href="#">Tables</a>	<a href="#">Figures</a>
<a href="#">◀</a>	<a href="#">▶</a>
<a href="#">◀</a>	<a href="#">▶</a>
<a href="#">Back</a>	<a href="#">Close</a>
<a href="#">Full Screen / Esc</a>	
<a href="#">Printer-friendly Version</a>	
<a href="#">Interactive Discussion</a>	



temperature using our steady-state model, we had to manually adjust  $f_{CA}$  for each incubation temperature. We will argue here that using different  $f_{CA}$  values on the same soil is justified given the way measurements were performed. VanDiest and Kesselmeier (2008) wanted to characterise the  $V_d$  response to soil drying at a set temperature and for this, they saturated a soil sample with water and acclimated it to a given temperature (between 5 and 35 °C), they then recorded the OCS exchange immediately and continued to measure until the soil was completely dry, this usually lasted 1 to 2 days. The same soil sample, or a different one from the same geographical location, was then re-watered and re-acclimated to a different temperature and another cycle of measurements started. Sometimes several months separated measurements at two different temperatures and/or different soil samples collected at different seasons were used. This means that, for a given soil origin, the microbial community was experiencing different environmental conditions and history between each drying curve. Thus, the size and diversity of the microbial population were likely different for each incubation temperature, thus justifying the use of different enhancement factors at each temperature.

Following this argument it seems that the optimum temperatures observed by VanDiest and Kesselmeier (2008) for different soil types are not a good proxy for the optimal temperature of CA activity ( $T_{opt,CA}$ ). Using our model we already showed that the optimum temperature for  $V_d$  ( $T_{opt,Vd}$ ) was different from  $T_{opt,CA}$ , at least for deep soils (Fig. 4). A closer inspection of the results shown in Figs. 9–12 also show that the adjusted  $f_{CA}$  values closely follow the patterns of the maximum  $V_d$  at  $\theta_{opt}$  (see right panels in Figs. 9–12). This means that the optimum temperature observed by Van Diest and Kesselmeier (2008) is a better indicator of maximum  $f_{CA}$  or equivalently maximum CA concentration (assuming all the CA's in the soil have similar  $k_{cat}/K_m$  as the pea extracts measured by Protoschill-Krebs et al., 1996). This could explain why the optimum for the German soil was so low (around 15 °C), i.e., lower than expected for  $T_{opt,CA}$ . The presence of a competing enzymatic process, such as OCS emission, could have explained this low  $T_{opt,Vd}$  value (Fig. 7) but it is more likely that the soil sample studied at 15 °C contained more CA than those used for other incubation temperatures. Mea-

[Title Page](#)[Abstract](#)[Introduction](#)[Conclusions](#)[References](#)[Tables](#)[Figures](#)[◀](#)[▶](#)[◀](#)[▶](#)[Back](#)[Close](#)[Full Screen / Esc](#)[Printer-friendly Version](#)[Interactive Discussion](#)

surements on microbial biomass could have helped confirm this hypothesis but were unfortunately not made.

Because  $f_{CA}$  is a fitting parameter in our model, it is important to see if the values that we derived for the different soils are realistic. There are two ways to do so. First, 5 we have a relatively good idea of how much CA is needed inside the cytosol of leaf mesophyll cells or in unicellular algae, of the order of 0.1 mM (Tholen and Zhu, 2011). Assuming this CA concentration value is also applicable to microbial cells, and using estimates of the soil microbial population size and Eq. (11) with the  $k_{cat}/K_m$  value for 10 OCS ( $2.39 \times 10^6 \text{ s}^{-1} \text{ M}^{-1}$  at  $20^\circ\text{C}$  and  $\text{pH}_{in}$  8.2) we can convert this physiological CA concentration into a CA concentration in the soil matrix and thus into an  $f_{CA}$ . With 15 a microbial population size of  $3 \times 10^9 \text{ cm}^{-3}$  and an average cell size of  $1 \mu\text{m}^3$ , this leads to an  $f_{CA}$  value of 36 000 for OCS, which is in the same order of magnitude as those found for the different soils in this study (between 21 600 and 336 000, with a median value at 66 000). Any increase in population size, the average cell size or 20 the physiological CA concentration would result in higher  $f_{CA}$  values. From this crude calculation we can conclude that our  $f_{CA}$  estimates are physiologically meaningful, at least for values below about 50 000.

Another way of checking if our  $f_{CA}$  estimates are meaningful is to convert them into  $f_{CA}$  equivalents for soil  $\text{CO}_2$  isotope fluxes, for which we have a better idea of what the 25 expected values should be (Seibt et al., 2006; Wingate et al., 2009, 2010, 2008). The  $k_{cat}/K_m$  value for  $\text{CO}_2$  in pea extracts has been measured for a pH range of 6–9 and at  $25^\circ\text{C}$  (Bjorkbacka et al., 1999). The pH response described a similar pattern as the one found for *Arabidopsis* by Rowlett et al. (2002) (Fig. 2) with a  $pK_a$  of 7.1. Using  $x_{CA}(T)$  and  $y_{CA}$  ( $\text{pH}_{in}$ ) to convert those values to  $\text{pH}_{in}$  8.2 and  $20^\circ\text{C}$ , we obtain a  $k_{cat}/K_m$  value for  $\text{CO}_2$  of  $50 \text{ s}^{-1} \mu\text{M}^{-1}$ , i.e., about 20 times greater than the  $k_{cat}/K_m$  for OCS. Given the difference in uncatalysed hydration rates between the two gas species ( $12\,000 \mu\text{s}^{-1}$  for  $\text{CO}_2$  and  $21.5 \mu\text{s}^{-1}$  for OCS at  $25^\circ\text{C}$  and  $\text{pH} = 4.5$ ) this means that at equal soil CA concentration, the  $f_{CA}$  for  $\text{CO}_2$  should be about 30 times smaller than that derived for OCS. This corresponds to a median  $f_{CA}$  value of 2200 for  $\text{CO}_2$ , i.e., at the higher end

[Title Page](#)[Abstract](#)[Introduction](#)[Conclusions](#)[References](#)[Tables](#)[Figures](#)[◀](#)[▶](#)[◀](#)[▶](#)[Back](#)[Close](#)[Full Screen / Esc](#)[Printer-friendly Version](#)[Interactive Discussion](#)

of values observed in different soils (Wingate et al., 2009). We can therefore draw the same conclusion as above, which is that the  $f_{CA}$  values obtained here for OCS are compatible with  $\text{CO}_2$  studies, but may be overestimated, by a factor two at least.

The calculation above considers only  $\beta$ -CA kinetic parameters to relate the soil CA enhancement factor for OCS to the  $f_{CA}$  for  $\text{CO}_2$ . However other enzymes can catalyse OCS hydrolysis and not have a strong affinity to  $\text{CO}_2$ . For example Smeulders et al. found a carbon disulphide hydrolase from an acido-thermophilic archaeon that was very efficient at catalysing OCS hydrolysis but did not have  $\text{CO}_2$  as one of its substrates (Smeulders et al., 2012). More recently, Ogawa et al. (2013) found in *Thiobacillus thioparus*, a sulfur-oxidizing bacterium widely distributed in soils and freshwaters, an enzyme that shared a high similarity with  $\beta$ -CAs and was able to catalyse OCS hydrolysis with a similar efficiency ( $K_m = 60 \mu\text{M}$ ,  $k_{\text{cat}} = 58 \text{ s}^{-1}$  at pH 8.5 and 30 °C) but whose  $\text{CO}_2$  hydration activity was 3–4 orders of magnitude smaller than that of  $\beta$ -CAs. For this reason they called this enzyme carbonyl sulphide hydrolase (COSase). The carbon disulphide hydrolase identified by Smeulders et al. (2012) may only be present in extremely acidic environments such as volcanic solfataras, but the COSase found in *T. thioparus* may be more ubiquitous in soils. If this was the case this would imply that the  $f_{CA}$  ratio of OCS to  $\text{CO}_2$  is not unique and could, in some soils, be higher than the same ratio derived from  $\beta$ -CA kinetic parameters only. This could partly explain the highest  $f_{CA}$  values obtained here for OCS.

Higher values of  $f_{CA}$  could also be explained by the fact that we neglected dispersion fluxes when we compared the model against observations. Indeed dispersion fluxes would enhance OCS diffusion (Eq. 15) and result in larger deposition velocities (Eq. 16b) for the same level of CA concentration. Results from Maier et al. (2012) show that the diffusivity  $D$  could be easily doubled by the presence of turbulence above the soil surface, which would be equivalent to a doubling of  $k$  ( $D$  and  $k$  appear as a product in the sink term of Eq. 16b). This means that the high  $f_{CA}$  values are probably overestimated by a factor two at least, bringing them closer to values compatible with physiological CA concentrations.

Title Page

Abstract

Introduction

Conclusions

References

Tables

Figures

◀

▶

◀

▶

Back

Close

Full Screen / Esc

Printer-friendly Version

Interactive Discussion



## 4.2 Can we transpose laboratory data to field conditions?

Response curves of OCS deposition rates to soil moisture and temperature have been derived from laboratory experiments similar to those presented here (Kesselmeier et al., 1999) and the derived equations have been used to estimate the OCS uptake by soils at the global scale (Kettle et al., 2002). Also Van Diest and Kesselmeier have proposed that the optimum soil moisture content for OCS deposition ( $\theta_{\text{opt}}$ ) was around  $0.12 \text{ m}^3 \text{ m}^{-3}$ , independently of soil type (Van Diest and Kesselmeier, 2008). Our model allows us to verify if such simplification or extrapolation is justified, on a theoretical point of view at least. From Fig. 4 we can see that the general shape of the soil moisture response and  $\theta_{\text{opt}}$  strongly depend on the exact soil depth used during the experiment, at least for soil less than 3 cm thick (or more if the CA activity is lower). For thicker soils the deepest soil layers do not contribute to the exchange and we reach the saturation point with soil weight shown in Fig. 5. However in both aforementioned studies (Kesselmeier et al., 1999; Van Diest and Kesselmeier, 2008), care was taken not to reach the saturation point (using soil weights of about 80 g). From our model results we can see that this would lead to an overestimation of  $\theta_{\text{opt}}$  and an overall underestimation of  $V_d$  (Fig. 4). Thus based on this observation we would recommend to use soil depths of at least 5–6 cm in future studies so that the results can be more readily extrapolated to field conditions.

Another difficulty when we want to extrapolate laboratory data to the natural environment is that soil disturbance prior to the experiment (sieving, repacking ...) strongly modifies the gas diffusivity properties of the soil. Our results show that OCS deposition rates can be extremely sensitive to the choice of the diffusivity model used (Fig. 3). In highly compacted, highly aggregated soils the gas diffusivity response to soil moisture content can even become bi-modal (Deepagoda et al., 2011) that would certainly have a strong impact on the  $V_d$ – $\theta$  relationship. Even without such a complication our results suggest that deposition rate measurements on repacked soils may not be representa-

[Title Page](#)[Abstract](#)[Introduction](#)[Conclusions](#)[References](#)[Tables](#)[Figures](#)[◀](#)[▶](#)[◀](#)[▶](#)[Back](#)[Close](#)[Full Screen / Esc](#)[Printer-friendly Version](#)[Interactive Discussion](#)

tive of field conditions because the soil treatment would modify the diffusivity properties of the soil and alter the soil moisture response of the OCS deposition rate.

BGD

12, 15687–15736, 2015

## 5 Perspectives

Our model so far has been tested under steady state conditions and with fairly uniform  
5 soil properties (temperature, moisture, pH...). In the natural environment such conditions are the exception rather than the rule. The model has not been tested either on true temperature response curves as happens in nature with strong diurnal variations of temperature at nearly constant soil moisture content. Indeed data from Van Diest and Kesselmeier (2008) have been collected at constant incubation temperatures and  
10 are therefore more indicative of the range of  $f_{CA}$  and  $V_d$  values one would expect over a growing season for a given soil type. Surprisingly we could not find published laboratory measurements of  $V_d$  where soil temperature was varied diurnally.

Another point that should be addressed in future studies is the characterisation of the soil microbial community size and structure, that should be done systematically with the soil OCS deposition measurements. This would allow us to test whether our  
15 upscaling of CA activity to the soil level (Eq. 11) is correct or not, and compatible with physiologically realistic CA contents in soil microbes. Our results so far suggest that the CA contents that we derive may be overestimated by a factor two at least, and the diffusivity model that we used may be partly responsible for it (see above). However  
20 having concurrent microbial data on the soil samples could greatly constrained our downscaling exercise and lead to a more precise picture of possible mismatch between our model and the observations. When combined with both OCS and  $CO_2$  isotope gas exchange measurements, it could also help identify the microbial communities that are more prone to express specific CAs which favor OCS uptake such as the COsase found in *T. thioparus*.

Finally our model has only been tested on oxic soils, although in theory, the model should also be able to predict OCS fluxes in anoxic soils. This would require mea-

Discussion Paper | Discussion Paper

Discussion Paper | Discussion Paper

Discussion Paper | Discussion Paper

A new mechanistic framework to predict OCS fluxes from soils

J. Ogée et al.

[Title Page](#)

[Abstract](#)

[Introduction](#)

[Conclusions](#)

[References](#)

[Tables](#)

[Figures](#)

◀

▶

◀

▶

[Back](#)

[Close](#)

[Full Screen / Esc](#)

[Printer-friendly Version](#)

[Interactive Discussion](#)



**A new mechanistic framework to predict OCS fluxes from soils**

J. Ogée et al.

[Title Page](#)[Abstract](#)[Introduction](#)[Conclusions](#)[References](#)[Tables](#)[Figures](#)[◀](#)[▶](#)[◀](#)[▶](#)[Back](#)[Close](#)[Full Screen / Esc](#)[Printer-friendly Version](#)[Interactive Discussion](#)

surements of soil redox potential, a measure nearly always missing from soil OCS flux studies, even when conducted on anoxic soils. Interestingly one study on boreal acidic soils reported higher rates of OCS uptake in water-logged plots compared to unsaturated plots (Simmons et al., 1999). This result seems to contradict most studies on anoxic soils that usually report OCS emissions (e.g., Fried et al., 1993; Hines and Morrison, 1992; Mello and Hines, 1994; Whelan et al., 2013), but our model may help explain this apparent contradiction. Indeed, provided that the saturation of the soil in the study by Simmons et al. (1999) was only recent (the experimental campaign lasted only 22 days and dry and wet conditions had been observed over that period), water logging could have induced a temporary rise in pH, thus enhancing CA activity (Fig. 2) and OCS uptake (Fig. 8). Had the water logging started several weeks before, the pH would have risen even further and may have reached more neutral conditions, but anoxic conditions would have also lowered the redox potential, leading to strong emissions of OCS, as observed in most other studies on anoxic soils. Our model can qualitatively explain this result and more generally how acidic soils can change from a sink to a source of OCS during water logging. It would be important in future studies to test whether the model is also good at describing this dynamic pattern quantitatively. This would open new possibilities to estimate OCS fluxes at large scales from both oxic and anoxic regions.

**Acknowledgements.** This work was funded by the European Research Council (ERC starting grant SOLCA), the French national research agency (ANR project ORCA) and the Institut National de la Recherche Agronomique (INRA PhD grant to J. Sauze).

## References

Beer, C., Reichstein, M., Tomelleri, E., Ciais, P., Jung, M., Carvalhais, N., Rödenbeck, C., Arain, M. A., Baldocchi, D., Bonan, G. B., Bondeau, A., Cescatti, A., Lasslop, G., Lindeiroth, A., Lomas, M., Luyssaert, S., Margolis, H., Oleson, K. W., Roupsard, O., Veenendaal, E., Viovy, N., Williams, C., Woodward, F. I., and Papale, D.: Terrestrial gross car-

bon dioxide uptake: global distribution and covariation with climate, *Science*, 329, 834–838, doi:10.1126/science.1184984, 2010.

Berry, J. A., Wolf, A., Campbell, J. E., Baker, I., Blake, N., Blake, D., Denning, A. S., Kawa, S. R., Montzka, S. A., Seibt, U., Stimler, K., Yakir, D., and Zhu, Z.: A coupled model of the global cycles of carbonyl sulfide and CO<sub>2</sub>: a possible new window on the carbon cycle, *J. Geophys. Res. Biogeosci.*, 118, 842–852, doi:10.1002/jgrg.20068, 2013.

Bird, R. B., Stewart, W. E., and Lightfoot, E. N.: *Transport Phenomena*, John Wiley & Sons, New York, 2002.

Bjorkbacka, H., Johansson, I.-M., and Forsman, C.: Possible roles for His 208 in the active-site region of chloroplast carbonic anhydrase from *Pisum sativum*, *Arch. Biochem. Biophys.*, 361, 17–24, 1999.

Blezinger, S., Wilhelm, C., and Kesselmeier, J.: Enzymatic consumption of carbonyl sulfide (COS) by marine algae, *Biogeochemistry*, 48, 185–197, 2000.

Bremner, J. M. and Banwart, W. L.: Sorption of sulfur gases by soils, *Soil Biol. Biochem.*, 8, 79–83, 1976.

Burnell, J. N. and Hatch, M. D.: Low bundle sheath carbonic anhydrase is apparently essential for effective C<sub>4</sub> pathway operation, *Plant Physiol.*, 86, 1252–1256, 1988.

Campbell, J. E., Carmichael, G. R., Chai, T., Mena-Carrasco, M., Tang, Y., Blake, D. R., Blake, N. J., Vay, S. A., Collatz, G. J., Baker, I., Berry, J. A., Montzka, S. A., Sweeney, C., Schnoor, J. L., and Stanier, C. O.: Photosynthetic control of atmospheric carbonyl sulfide during the growing season, *Science*, 322, 1085–1088, doi:10.1126/science.1164015, 2008.

Castro, M. S. and Galloway, J. N.: A comparison of sulfur-free and ambient air enclosure techniques for measuring the exchange of reduced sulfur gases between soils and the atmosphere, *J. Geophys. Res.-Atmos.*, 96, 15427–15437, 1991.

Choi, J.-G., Do, D. D., and Do, H. D.: Surface diffusion of adsorbed molecules in porous media: monolayer, multilayer, and capillary condensation regimes, *Ind. Eng. Chem. Res.*, 40, 4005–4031, doi:10.1021/ie010195z, 2001.

De Bruyn, W. J., Swartz, E., Hu, J. H., Shorter, J. A., Davidovits, P., Worsnop, D. R., Zahner, M. S., and Kolb, C. E.: Henry's law solubilities and Šetchenow coefficients for biogenic reduced sulfur species obtained from gas-liquid uptake measurements, *J. Geophys. Res.-Atmos.*, 100, 7245–7251, 1995.

**A new mechanistic framework to predict OCS fluxes from soils**

J. Ogée et al.

[Title Page](#)[Abstract](#)[Introduction](#)[Conclusions](#)[References](#)[Tables](#)[Figures](#)[|◀](#)[▶|](#)[◀](#)[▶](#)[Back](#)[Close](#)[Full Screen / Esc](#)[Printer-friendly Version](#)[Interactive Discussion](#)

Deepagoda, T. K. K. C., Moldrup, P., Schjønning, P., de Jonge, L. W., Kawamoto, K., and Komatsu, T.: Density-corrected models for gas diffusivity and air permeability in unsaturated soil, *Vadose Zone J.*, 10, 226–238, doi:10.2136/vzj2009.0137, 2011.

Delaune, R. D. and Reddy, K. R.: Redox potential, in: *Encyclopedia of Soils in the Environment*, edited by: D. Hillel, Academic Press/Elsevier B.V., New York, 366–371, 2005.

Devai, I. and Delaune, R. D.: Formation of volatile sulfur compounds in salt marsh sediment as influenced by soil redox condition, *Org. Geochem.*, 23, 283–287, 1995.

Elliott, S., Lu, E., and Rowland, F. S.: Rates and mechanisms for the hydrolysis of carbonyl sulfide in natural waters, *Environ. Sci. Technol.*, 23, 458–461, doi:10.1021/es00181a011, 1989.

Evans, J. R., Kaldenhoff, R., Genty, B., and Terashima, I.: Resistances along the CO<sub>2</sub> diffusion pathway inside leaves, *J. Exp. Bot.*, 60, 2235–2248, doi:10.1093/jxb/erp117, 2009.

Falta, R. W., Javandel, I., Pruess, K., and Witherspoon, P. A.: Density-driven flow of gas in the unsaturated zone due to the evaporation of volatile organic-compounds, *Water Resour. Res.*, 25, 2159–2169, 1989.

Frankenberg, C., Fisher, J. B., Worden, J., Badgley, G., Saatchi, S. S., Lee, J.-E., Toon, G. C., Butz, A., Jung, M., Kuze, A., and Yokota, T.: New global observations of the terrestrial carbon cycle from GOSAT: patterns of plant fluorescence with gross primary productivity, *Geophys. Res. Lett.*, 38, L17706, doi:10.1029/2011GL048738, 2011.

Fried, A., Klinger, L. F., and Erickson III, D. J.: Atmospheric carbonyl sulfide exchange in bog microcosms, *Geophys. Res. Lett.*, 20, 129–132, 1993.

Friedlingstein, P., Bopp, L., Rayner, P., Cox, P. M., Betts, R., Jones, C., Bloh, Von, W., Brovkin, V., Cadule, P., and Doney, S. C.: Climate-carbon cycle feedback analysis: results from the C4MIP model intercomparison, *J. Climate*, 19, 3337–3353, 2006.

Gurney, K. R. and Eckels, W. J.: Regional trends in terrestrial carbon exchange and their seasonal signatures, *Tellus B*, 63, 328–339, doi:10.1111/j.1600-0889.2011.00534.x, 2011.

Haritos, V. S. and Dojchinov, G.: Carbonic anhydrase metabolism is a key factor in the toxicity of CO<sub>2</sub> and COS but not CS<sub>2</sub> toward the flour beetle *Tribolium castaneum* [Coleoptera: Tenebrionidae], *Comp. Biochem. Phys. C*, 140, 139–147, doi:10.1016/j.cca.2005.01.012, 2005.

Hines, M. E. and Morrison, M. C.: Emissions of biogenic sulfur gases from Alaskan tundra, *J. Geophys. Res.*, 97, 16–703–16–707, 1992.

[Title Page](#)[Abstract](#)[Introduction](#)[Conclusions](#)[References](#)[Tables](#)[Figures](#)[◀](#)[▶](#)[◀](#)[▶](#)[Back](#)[Close](#)[Full Screen / Esc](#)[Printer-friendly Version](#)[Interactive Discussion](#)

Husson, O.: Redox potential (Eh) and pH as drivers of soil/plant/microorganism systems: a transdisciplinary overview pointing to integrative opportunities for agronomy, *Plant Soil*, 362, 389–417, doi:10.1007/s11104-012-1429-7, 2012.

5 Isik, S., Kockar, F., Aydin, M., Arslan, O., Guler, O. O., Innocenti, A., Scozzafava, A., and Supuran, C. T.: Carbonic anhydrase inhibitors: inhibition of the beta-class enzyme from the yeast *Saccharomyces cerevisiae* with sulfonamides and sulfamates, *Bioorgan. Med. Chem.*, 17, 1158–1163, doi:10.1016/j.bmc.2008.12.035, 2009.

10 Kesselmeier, J., Teusch, N., and Kuhn, U.: Controlling variables for the uptake of atmospheric carbonyl sulfide by soil, *J. Geophys. Res.*, 104, 11,577–11,584, 1999.

15 Kettle, A. J., Kuhn, U., Hobe, von, M., Kesselmeier, J., and Andreae, M. O.: Global budget of atmospheric carbonyl sulfide: temporal and spatial variations of the dominant sources and sinks, *J. Geophys. Res.*, 107, 4658, doi:10.1029/2002JD002187, 2002.

Krulwich, T. A., Sachs, G., and Padan, E.: Molecular aspects of bacterial pH sensing and homeostasis, *Nat. Rev. Microbiol.*, 9, 330–343, doi:10.1038/nrmicro2549, 2011.

20 15 Kuhn, U., Ammann, C., Wolf, A., Meixner, F., Andreae, M., and Kesselmeier, J.: Carbonyl sulfide exchange on an ecosystem scale: soil represents a dominant sink for atmospheric COS, *Atmos. Environ.*, 33, 995–1008, 1999.

Launois, T., Peylin, P., Belviso, S., and Poulter, B.: A new model of the global biogeochemical cycle of carbonyl sulfide – Part 2: Use of carbonyl sulfide to constrain gross primary productivity in current vegetation models, *Atmos. Chem. Phys.*, 15, 9285–9312, doi:10.5194/acp-15-9285-2015, 2015.

25 Liu, J., Geng, C., Mu, Y., Zhang, Y., Xu, Z., and Wu, H.: Exchange of carbonyl sulfide (COS) between the atmosphere and various soils in China, *Biogeosciences*, 7, 753–762, doi:10.5194/bg-7-753-2010, 2010.

Liu, Y., He, H., and Ma, Q.: Temperature dependence of the heterogeneous reaction of carbonyl sulfide on magnesium oxide, *J. Phys. Chem. A*, 112, 2820–2826, doi:10.1021/jp711302r, 2008.

30 Liu, Y., Ma, Q., and He, H.: Comparative study of the effect of water on the heterogeneous reactions of carbonyl sulfide on the surface of  $\alpha$ -Al<sub>2</sub>O<sub>3</sub> and MgO, *Atmos. Chem. Phys.*, 9, 6273–6286, doi:10.5194/acp-9-6273-2009, 2009.

Liu, Y., Ma, J., and He, H.: Heterogeneous reactions of carbonyl sulfide on mineral oxides: mechanism and kinetics study, *Atmos. Chem. Phys.*, 10, 10335–10344, doi:10.5194/acp-10-10335-2010, 2010a.

A new mechanistic framework to predict OCS fluxes from soils

J. Ogée et al.

[Title Page](#)

[Abstract](#)

[Introduction](#)

[Conclusions](#)

[References](#)

[Tables](#)

[Figures](#)

◀

▶

◀

▶

[Back](#)

[Close](#)

[Full Screen / Esc](#)

[Printer-friendly Version](#)

[Interactive Discussion](#)



Liu, Y., Ma, J., Liu, C., and He, H.: Heterogeneous uptake of carbonyl sulfide onto kaolinite within a temperature range of 220–330 K, *J. Geophys. Res.*, 115, D24311, doi:10.1029/2010JD014778, 2010b.

5 Maier, M., Schack-Kirchner, H., Aubinet, M., Goffin, S., Longdoz, B., and Parent, F.: Turbulence effect on gas transport in three contrasting forest soils, *Soil Sci. Soc. Am. J.*, 76, 1518, doi:10.2136/sssaj2011.0376, 2012.

Manzoni, S. and Katul, G. G.: Invariant soil water potential at zero microbial respiration explained by hydrological discontinuity in dry soils, *Geophys. Res. Lett.*, 41, 7151–7158, doi:10.1002/(ISSN)1944-8007, 2014.

10 Maseyk, K., Berry, J. A., Billesbach, D., Campbell, J. E., Torn, M. S., Zahniser, M., and Seibt, U.: Sources and sinks of carbonyl sulfide in an agricultural field in the Southern Great Plains, *P. Natl. Acad. Sci. USA*, 111, 9064–9069, doi:10.1073/pnas.1319132111, 2014.

Massman, W. J.: A review of the molecular diffusivities of  $H_2O$ ,  $CO_2$ ,  $CH_4$ ,  $CO$ ,  $O_3$ ,  $SO_2$ ,  $NH_3$ ,  $N_2O$ ,  $NO$ , and  $NO_2$  in air,  $O_2$  and  $N_2$  near STP, *Atmos. Environ.*, 32, 1111–1127, 1998.

15 Massman, W. J., Sommerfeld, R. A., Mosier, A. R., Zeller, K. F., Hehn, T. J., and Rochelle, S. G.: A model investigation of turbulence-driven pressure-pumping effects on the rate of diffusion of  $CO_2$ ,  $N_2O$ , and  $CH_4$  through layered snowpacks, *J. Geophys. Res.-Atmos.*, 102, 18851–18863, 1997.

Mello, W. Z. and Hines, M. E.: Application of static and dynamic enclosures for determining 20 dimethyl sulfide and carbonyl sulfide exchange in *Sphagnum* peatlands: implications for the magnitude and direction of flux, *J. Geophys. Res.*, 99, 14-601–14-607, 1994.

Merlin, C., Masters, M., McAteer, S., and Coulson, A.: Why is carbonic anhydrase essential to *Escherichia coli*?, *J. Bacteriol.*, 185, 6415–6424, doi:10.1128/JB.185.21.6415-6424.2003, 2003.

25 Millington, R. J. and Quirk, J. P.: Permeability of porous solids, *T. Faraday Soc.*, 57, 1200–1207, 1961.

Moldrup, P., Olesen, T., Komatsu, T., Yoshikawa, S., Schjønning, P., and Rolston, D. E.: Modeling diffusion and reaction in soils: X. A unifying model for solute and gas diffusivity in unsaturated soil, *Soil Sci.*, 168, 321–337, doi:10.1097/00010694-200305000-00002, 2003.

30 Montzka, S. A., Calvert, P., Hall, B. D., Elkins, J. W., Conway, T. J., Tans, P. P., and Sweeney, C.: On the global distribution, seasonality, and budget of atmospheric carbonyl sulfide (COS) and some similarities to  $CO_2$ , *J. Geophys. Res.*, 112, D09302, doi:10.1029/2006JD007665, 2007.

Title Page

Abstract

Introduction

Conclusions

References

Tables

Figures

◀

▶

◀

▶

Back

Close

Full Screen / Esc

Printer-friendly Version

Interactive Discussion



## A new mechanistic framework to predict OCS fluxes from soils

J. Ogée et al.

[Title Page](#)

[Abstract](#)

[Introduction](#)

[Conclusions](#)

[References](#)

[Tables](#)

[Figures](#)

◀

▶

◀

▶

[Back](#)

[Close](#)

[Full Screen / Esc](#)

[Printer-friendly Version](#)

[Interactive Discussion](#)



corrected by deposition velocities normalized to the uptake of carbon dioxide (CO<sub>2</sub>), *Biogeosciences*, 2, 125–132, doi:10.5194/bg-2-125-2005, 2005.

Scanlon, B. R., Nicot, J. P., and Massmann, J. W.: Soil gas movement in unsaturated systems, in: *Soil Physics Companion*, CRC Press, Boca Raton, FL, 297–341, 2002.

5 Seibt, U., Wingate, L., Lloyd, J., and Berry, J. A.: Diurnally variable  $\delta^{18}\text{O}$  signatures of soil CO<sub>2</sub> fluxes indicate carbonic anhydrase activity in a forest soil, *J. Geophys. Res.*, 111, G04005, doi:10.1029/2006JG000177, 2006.

10 Seibt, U., Kesselmeier, J., Sandoval-Soto, L., Kuhn, U., and Berry, J. A.: A kinetic analysis of leaf uptake of COS and its relation to transpiration, photosynthesis and carbon isotope fractionation, *Biogeosciences*, 7, 333–341, doi:10.5194/bg-7-333-2010, 2010.

Simmons, J. S., Klemedtsson, L., Hultber, H., and Hines, M. E.: Consumption of atmospheric carbonyl sulfide by coniferous forest soils, *J. Geophys. Res.*, 104, 11–569–11–576, 1999.

15 Smeulders, M. J., Barends, T. R. M., Pol, A., Scherer, A., Zandvoort, M. H., Udvarhelyi, A., Khadem, A. F., Menzel, A., Hermans, J., Shoeman, R. L., Wessels, H. J. C. T., van den Heuvel, L. P., Russ, L., Schlichting, I., Jetten, M. S. M., and Op den Camp, H. J. M.: Evolution of a new enzyme for carbon disulphide conversion by an acidothermophilic archaeon, *Nature*, 478, 412–416, doi:10.1038/nature10464, 2012.

Smith, K., Jakubzick, C., Whittam, T., and Ferry, J.: Carbonic anhydrase is an ancient enzyme widespread in prokaryotes, *P. Natl. Acad. Sci. USA*, 96, 15184–15189, 1999.

20 Steinbacher, M., Bingemer, H., and Schmidt, U.: Measurements of the exchange of carbonyl sulfide (OCS) and carbon disulfide (CS<sub>2</sub>) between soil and atmosphere in a spruce forest in central Germany, *Atmos. Environ.*, 38, 6043–6052, doi:10.1016/j.atmosenv.2004.06.022, 2004.

25 Stimler, K., Montzka, S. A., Berry, J. A., Rudich, Y., and Yakir, D.: Relationships between carbonyl sulfide (COS) and CO<sub>2</sub> during leaf gas exchange, *New Phytol.*, 186, 869–878, doi:10.1111/j.1469-8137.2010.03218.x, 2010.

Stimler, K., Berry, J. A., and Yakir, D.: Effects of carbonyl sulfide and carbonic anhydrase on stomatal conductance, *Plant Physiol.*, 158, 524–530, doi:10.1104/pp.111.185926, 2012.

30 Sun, W., Maseyk, K., Lett, C., and Seibt, U.: A soil diffusion-reaction model for surface COS flux: COSSM v1, *Geosci. Model Dev. Discuss.*, 8, 5139–5182, doi:10.5194/gmdd-8-5139-2015, 2015.

Syrjänen, L., Vermelho, A. B., de Almeida Rodrigues, I., Corte-Real, S., Salonen, T., Pan, P., Vullo, D., Parkkila, S., Capasso, C., and Supuran, C. T.: Cloning, characteriza-

Title Page

Abstract

Introduction

Conclusions

References

Tables

Figures

|◀

▶|

◀

▶

Back

Close

Full Screen / Esc

Printer-friendly Version

Interactive Discussion



tion, and inhibition studies of a  $\beta$ -carbonic anhydrase from *Leishmania donovani chagasi*, the protozoan parasite responsible for leishmaniasis, *J. Med. Chem.*, 56, 7372–7381, doi:10.1021/jm400939k, 2013.

5 Tholen, D. and Zhu, X.-G.: The mechanistic basis of internal conductance: a theoretical analysis of mesophyll cell photosynthesis and  $\text{CO}_2$  diffusion, *Plant Physiol.*, 156, 90–105, doi:10.1104/pp.111.172346, 2011.

Ulshöfer, V. S., Flock, O. R., Uher, G., and Andreae, M. O.: Photochemical production and air-sea exchange of carbonyl sulfide in the eastern Mediterranean Sea, *Mar. Chem.*, 53, 25–39, 1996.

10 van Bochove, E., Beauchemin, S., and Thériault, G.: Continuous multiple measurement of soil redox potential using platinum microelectrodes, *Soil Sci. Soc. Am. J.*, 66, 1813–1820, 2002.

Van Diest, H. and Kesselmeier, J.: Soil atmosphere exchange of carbonyl sulfide (COS) regulated by diffusivity depending on water-filled pore space, *Biogeosciences*, 5, 475–483, doi:10.5194/bg-5-475-2008, 2008.

15 Welp, L. R., Keeling, R. F., Meijer, H. A. J., Bollenbacher, A. F., Piper, S. C., Yoshimura, K., Francey, R. J., Allison, C. E., and Wahlen, M.: Interannual variability in the oxygen isotopes of atmospheric  $\text{CO}_2$  driven by El Niño, *Nature*, 477, 579–582, doi:10.1038/nature10421, 2011.

Whelan, M. E. and Rhew, R. C.: Carbonyl sulfide produced by abiotic thermal and photodegradation of soil organic matter from wheat field substrate, *J. Geophys. Res. Biogeosci.*, 120, 54–62, doi:10.1002/2014JG002661, 2015.

20 Whelan, M. E., Min, D.-H., and Rhew, R. C.: Salt marsh vegetation as a carbonyl sulfide (COS) source to the atmosphere, *Atmos. Environ.*, 73, 131–137, doi:10.1016/j.atmosenv.2013.02.048, 2013.

25 White, M. L., Zhou, Y., Russo, R. S., Mao, H., Talbot, R., Varner, R. K., and Sive, B. C.: Carbonyl sulfide exchange in a temperate loblolly pine forest grown under ambient and elevated  $\text{CO}_2$ , *Atmos. Chem. Phys.*, 10, 547–561, doi:10.5194/acp-10-547-2010, 2010.

Wilhelm, E., Battino, R., and Wilcock, R. J.: Low-pressure solubility of gases in liquid water, *Chem. Rev.*, 77, 219–262, 1977.

30 Wingate, L., Seibt, U., Maseyk, K., Ogée, J., Almeida, P., Yakir, D., Pereira, J. S., and Menuccini, M.: Evaporation and carbonic anhydrase activity recorded in oxygen isotope signatures of net  $\text{CO}_2$  fluxes from a Mediterranean soil, *Global Change Biol.*, 14, 2178–2193, doi:10.1111/j.1365-2486.2008.01635.x, 2008.

[Title Page](#)

[Abstract](#)

[Introduction](#)

[Conclusions](#)

[References](#)

[Tables](#)

[Figures](#)

◀

▶

◀

▶

[Back](#)

[Close](#)

[Full Screen / Esc](#)

[Printer-friendly Version](#)

[Interactive Discussion](#)



<a href="#">Title Page</a>	
<a href="#">Abstract</a>	<a href="#">Introduction</a>
<a href="#">Conclusions</a>	<a href="#">References</a>
<a href="#">Tables</a>	<a href="#">Figures</a>
 	 
<a href="#">Back</a>	<a href="#">Close</a>
<a href="#">Full Screen / Esc</a>	
<a href="#">Printer-friendly Version</a>	
<a href="#">Interactive Discussion</a>	



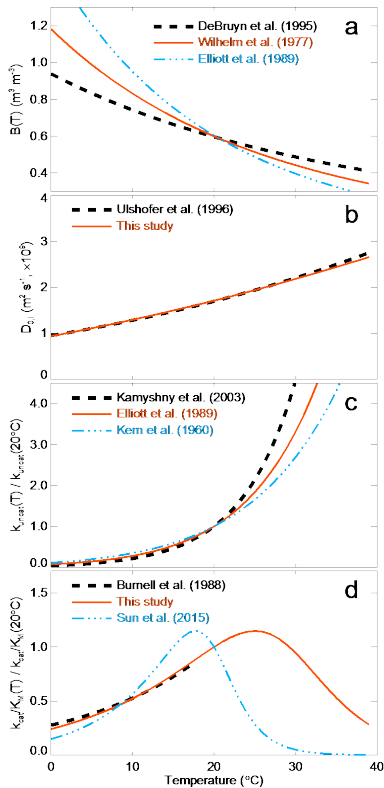


**Figure 1.** Temperature response of **(a)** the OCS solubility in water, **(b)** the OCS diffusivity in liquid water and **(c)** the uncatalysed and **(d)** CA-catalysed OCS hydrolysis rates. Red lines indicate the parameterisation used for this study.

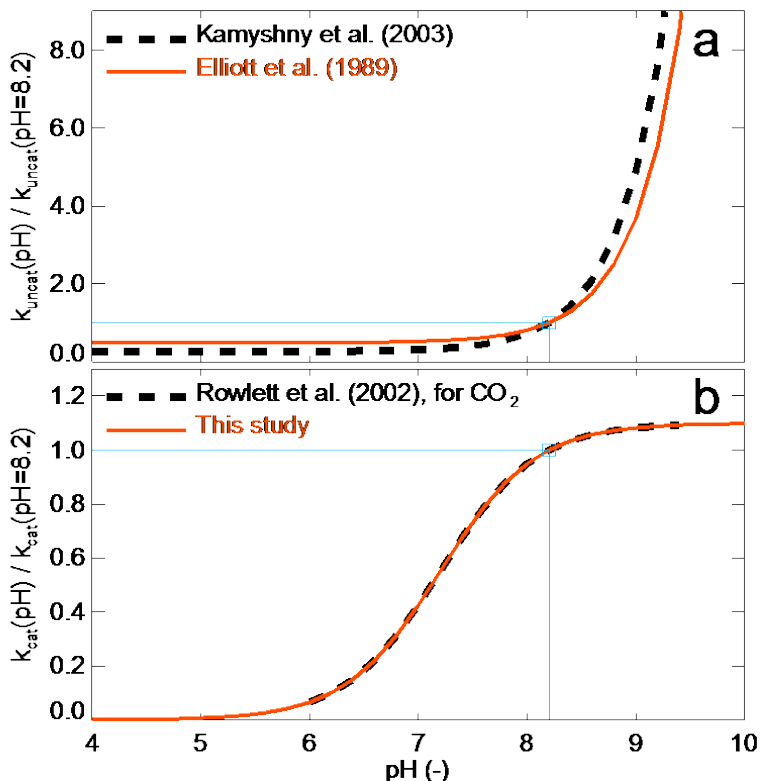


**Figure 2.** Response of the **(a)** uncatalysed and **(b)** CA-catalysed OCS hydrolysis rates to changes in soil pH. Red lines indicate the parameterisation used for this study. The blue lines indicate the normalisation at pH = 8.2.

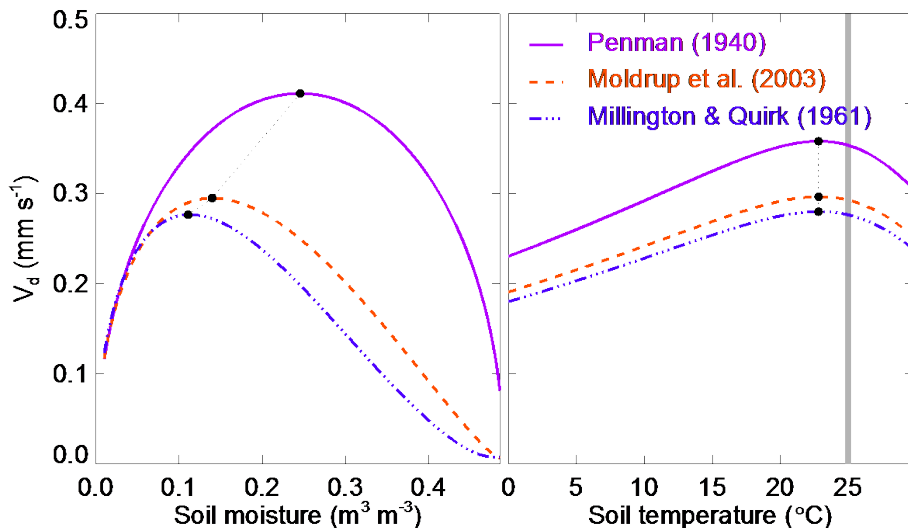


**Figure 3.** Sensitivity of the modelled OCS deposition velocity to the formulation used to describe gaseous and solute diffusion. The soil moisture and temperature response curves shown here were obtained assuming no source term, a soil depth and pH of 1 m and 7.2 respectively and a CA enhancement factor for OCS hydrolysis of 30 000. Closed circles indicate the temperature or soil moisture optimum of each response curve and the grey thick line in left panel indicates the set optimal temperature for CA activity (25 °C in this case).

- [Title Page](#)
- [Abstract](#) [Introduction](#)
- [Conclusions](#) [References](#)
- [Tables](#) [Figures](#)
- [◀](#) [▶](#)
- [◀](#) [▶](#)
- [Back](#) [Close](#)
- [Full Screen / Esc](#)
- [Printer-friendly Version](#)
- [Interactive Discussion](#)

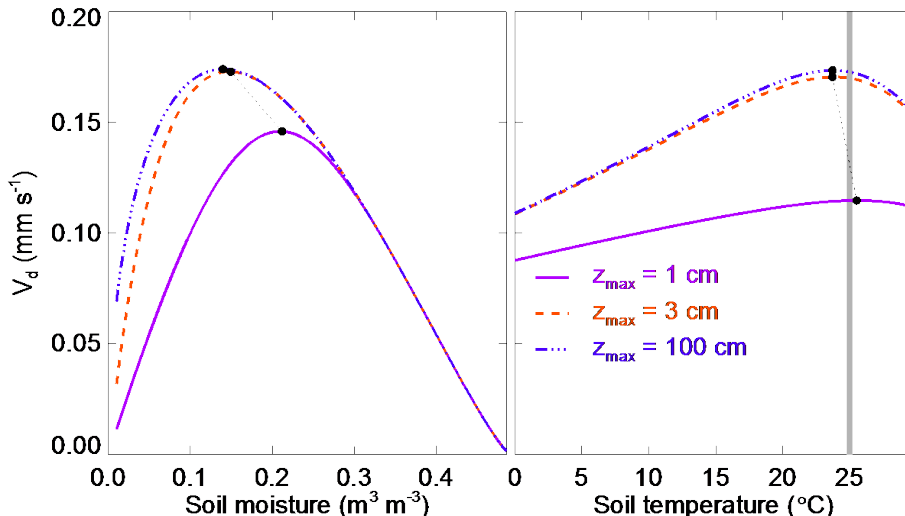


**Figure 4.** Sensitivity of the modelled OCS deposition velocity to soil column depth. The soil moisture and temperature response curves shown here were obtained using the diffusivity model of Moldrup et al. (2003) and assuming no source term, a soil pH of 7.2 and a CA enhancement factor for OCS hydrolysis of 30 000. Closed circles indicate the temperature or soil moisture optimum of each response curve and the grey thick line in left panel indicates the set optimal temperature for CA activity (25 °C in this case).

- [Title Page](#)
- [Abstract](#) [Introduction](#)
- [Conclusions](#) [References](#)
- [Tables](#) [Figures](#)
- [◀](#) [▶](#)
- [◀](#) [▶](#)
- [Back](#) [Close](#)
- [Full Screen / Esc](#)
- [Printer-friendly Version](#)
- [Interactive Discussion](#)

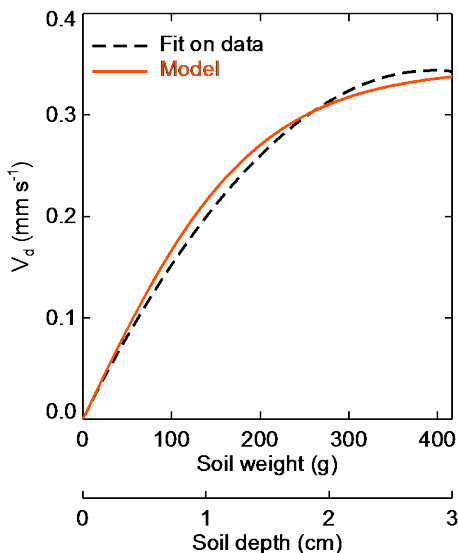


**Figure 5.** Modelled (solid line) and observed (dotted line) response of the modelled OCS deposition velocity to soil column depth. Soil column depth is also converted into soil weight assuming a soil surface area of  $165.1\text{ cm}^2$  and a soil bulk density and pH of  $0.85\text{ kg m}^{-3}$  and 7.2, respectively, to be comparable with the experimental setup used in Kesselmeier et al. (1999) to derive the observed response curve. Model results shown here were obtained using the diffusivity model of Moldrup et al. (2003) and assuming an enhancement factor and an optimum temperature for OCS hydrolysis of 26 000 and  $25\text{ }^\circ\text{C}$ , respectively and no source term. Soil water content and temperature were also set to 11 % weight and  $17\text{ }^\circ\text{C}$ , respectively, to be comparable with the experimental data, while the fit on observed uptake rates that was originally reported were converted into deposition velocities assuming a constant mixing ratio of 600 ppt (Kesselmeier et al., 1999).

<a href="#">Title Page</a>	<a href="#">Abstract</a>	<a href="#">Introduction</a>
<a href="#">Conclusions</a>	<a href="#">References</a>	
<a href="#">Tables</a>	<a href="#">Figures</a>	
<a href="#">◀</a>	<a href="#">▶</a>	
<a href="#">◀</a>	<a href="#">▶</a>	
<a href="#">Back</a>	<a href="#">Close</a>	
<a href="#">Full Screen / Esc</a>		
	<a href="#">Printer-friendly Version</a>	
	<a href="#">Interactive Discussion</a>	

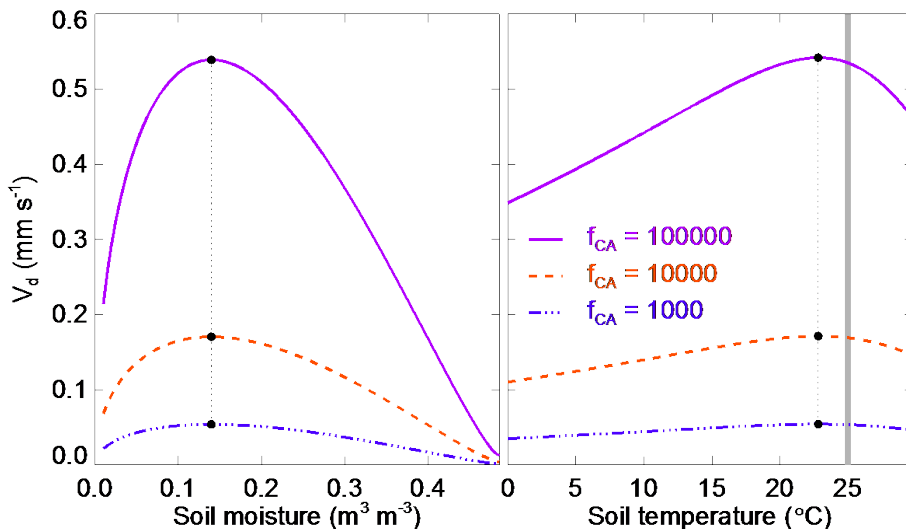


**Figure 6.** Sensitivity of the modelled OCS deposition velocity to soil CA activity. The soil moisture and temperature response curves shown here were obtained using the diffusivity model of Moldrup et al. (2003) and assuming no source term, a soil pH of 7.2 and a soil depth of 1 m. Closed circles indicate the temperature or soil moisture optimum of each response curve and the grey thick line in left panel indicates the set optimal temperature for CA activity (25 °C in this case).

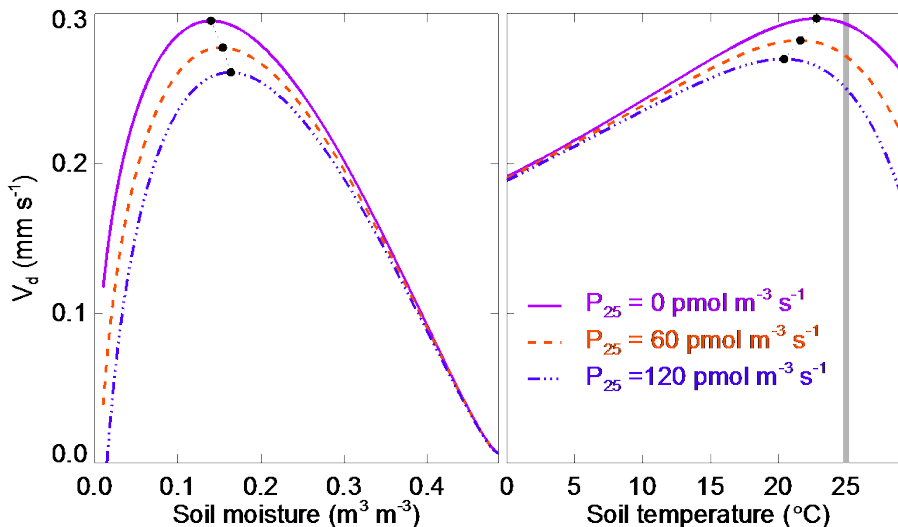


**Figure 7.** Sensitivity of the modelled OCS deposition velocity to soil OCS emission rate. The soil moisture and temperature response curves shown here were obtained using the diffusivity model of Moldrup et al. (2003) and assuming a CA enhancement factor of 30 000, a soil pH of 7.2 and a soil depth of 1 m. OCS source is assumed to occur only in the top 5 cm. Closed circles indicate the temperature or soil moisture optimum of each response curve and the grey thick line in left panel indicates the set optimal temperature for CA activity (25 °C in this case).

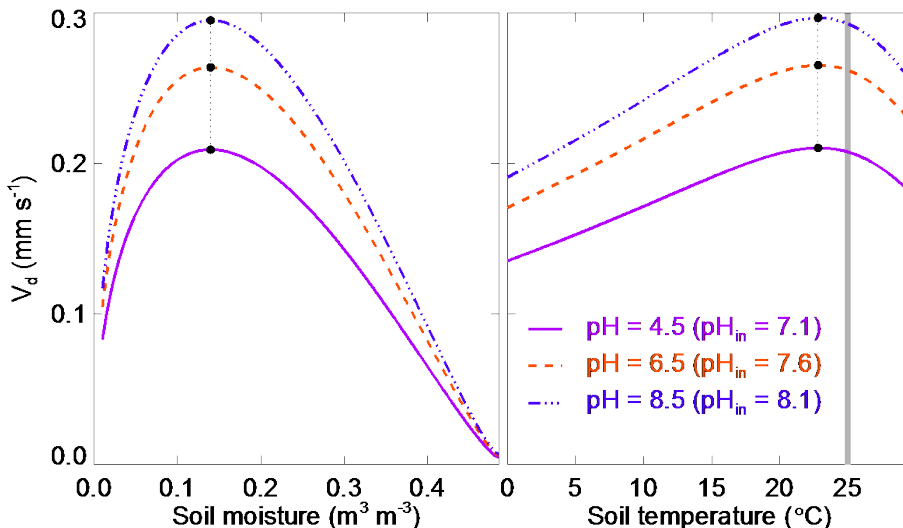


**Figure 8.** Sensitivity of the modelled OCS deposition velocity to soil pH. The soil moisture and temperature response curves shown here were obtained using the diffusivity model of Moldrup et al. (2003) and assuming no source term, a CA concentration in the soil of 330 nM and a soil depth of 1 m. Closed circles indicate the temperature or soil moisture optimum of each response curve and the grey thick line in left panel indicates the set optimal temperature for CA activity (25 °C in this case).

## A new mechanistic framework to predict OCS fluxes from soils

J. Ogée et al.

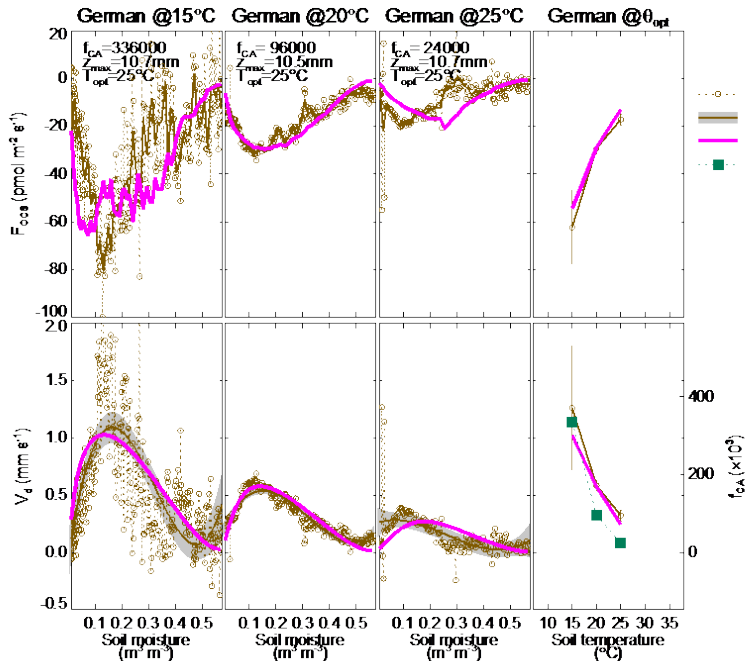


**Figure 9.** Observed and modelled soil–air OCS flux and deposition velocity during soil drying at different incubation temperatures (indicated above each panel) and their value at a soil moisture content  $W_{\text{opt}} = 0.12 \text{ cm}^3 \text{ cm}^{-3}$  (far right panels). The soil moisture and temperature response curves shown here were recalculated from data of VanDiest and Kesselmeier (2008) (open circles and brown line) or computed with our model (thick pink line) using the diffusivity model of Moldrup et al. (2003). For each incubation temperature, a different set of model parameters ( $f_{\text{CA}}$ ,  $Z_{\text{max}}$ ,  $T_{\text{opt}}$ ) was used as indicated in each panel. The data shown here are representative of an agricultural soil near Mainz in Germany (soil weight is 200 g).

## A new mechanistic framework to predict OCS fluxes from soils

J. Ogée et al.

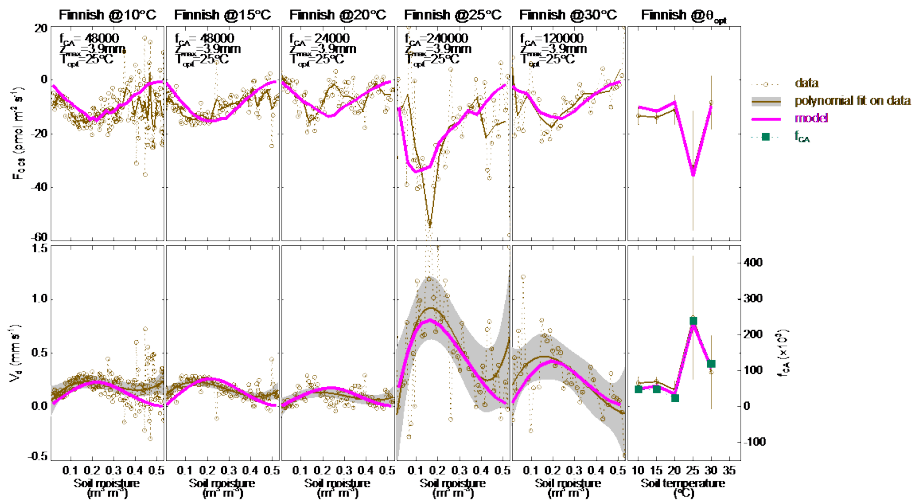


**Figure 10.** Same as Fig. 9 but for an agricultural soil near Hyttiala in Finland (soil weight is 80 g).

- [Title Page](#)
- [Abstract](#) [Introduction](#)
- [Conclusions](#) [References](#)
- [Tables](#) [Figures](#)
- [◀](#) [▶](#)
- [◀](#) [▶](#)
- [Back](#) [Close](#)
- [Full Screen / Esc](#)
- [Printer-friendly Version](#)
- [Interactive Discussion](#)

## A new mechanistic framework to predict OCS fluxes from soils

J. Ogée et al.

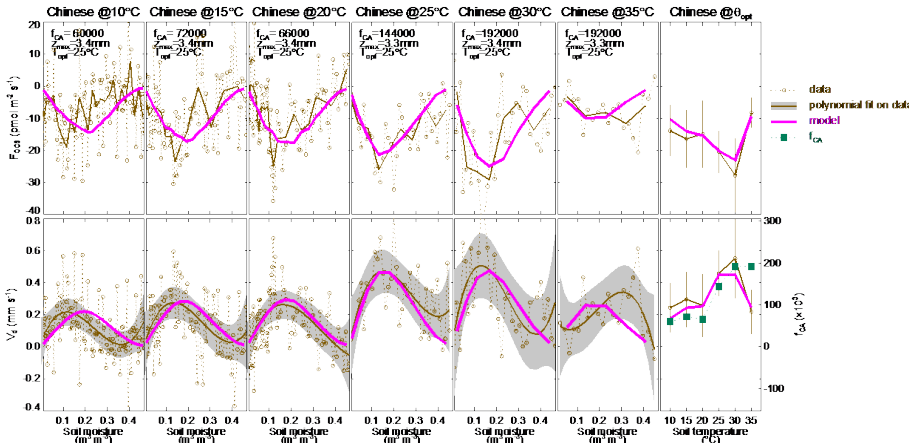


**Figure 11.** Same as Fig. 9 but for an agricultural soil from north-eastern China (soil weight is 80 g).

[Title Page](#)

[Abstract](#)

[Introduction](#)

[Conclusions](#)

[References](#)

[Tables](#)

[Figures](#)

◀

▶

◀

▶

[Back](#)

[Close](#)

[Full Screen / Esc](#)

[Printer-friendly Version](#)

[Interactive Discussion](#)

## A new mechanistic framework to predict OCS fluxes from soils

J. Ogée et al.

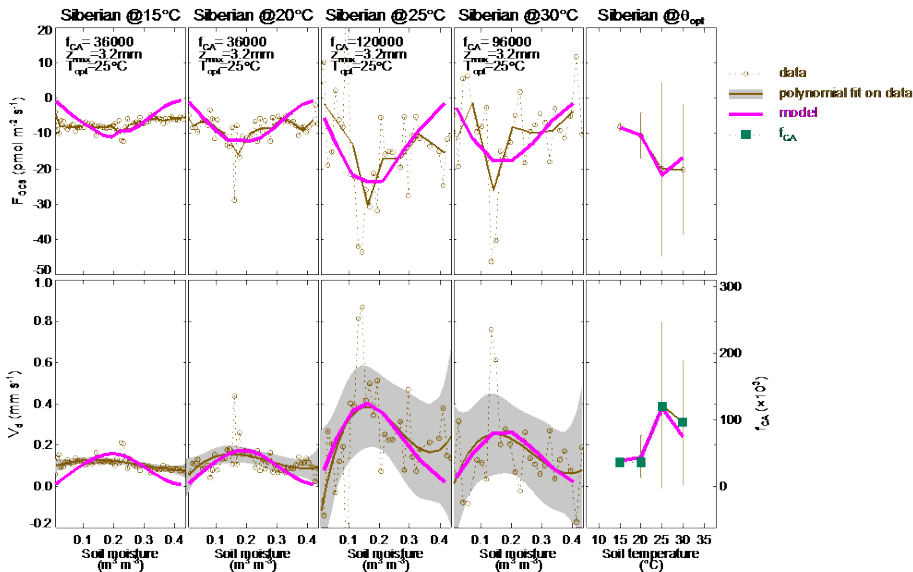


**Figure 12.** Same as Fig. 9 but for an agricultural soil from Siberia (soil weight is 80 g).